Molecular Phylogenetics and Evolution 204 (2025) 108242

Contents lists available at ScienceDirect

Molecular Phylogenetics and Evolution

journal homepage: www.elsevier.com/locate/ympev

Evolution, range formation and a revised taxonomy of the disjunctly distributed European members of *Astragalus* sect. *Caprini*, an intricate group including highly endangered species of dry grasslands

Clemens Maylandt [a], Philipp Kirschner [a], Daniela Pirkebner [a], Božo Frajman [a], Julio Peñas de Giles [b], Peter Schönswetter [a,*], Pau Carnicero [a,*]

[a] Department of Botany, University of Innsbruck, Sternwartestr. 15, 6020 Innsbruck, Austria
[b] Botany Department, University of Granada, 18071 Granada, Spain

ARTICLE INFO

Keywords:
Eurasian steppe
Pleistocene
RADseq
Warm-stage refugium
Secondary contact

ABSTRACT

The Eurasian steppes are among the largest and most threatened biomes on Earth. During cold periods of the Pleistocene, the zonal Eurasian steppes had a much larger extent as compared to interglacial periods, and repeatedly expanded into large areas of present-day forested temperate Europe. Conversely, during warm periods, forest expansion recurrently forced Eurasian steppe biota into disjunct and small warm-stage refugia, i.e. today's extrazonal steppes. The rare, threatened and disjunctly distributed northwestern African and European members of *Astragalus* sect. *Caprini* constitute an ideal model for gaining insights into the evolutionary dynamics of typical steppe biota. Here, we reconstructed the spatiotemporal diversification of northwestern African and European members of *Astragalus* sect. *Caprini* based on a combination of RADseq data, single gene markers (internal transcribed spacer, plastid *ycf1*), genome size measurements and multivariate morphometrics. We outline an evolutionary scenario in which the group originated in the Irano-Turanian region and started to diversify shortly after the Mid-Pleistocene-Transition (ca. 0.5 to 0.7 Ma). While lineages occurring in (sub-) mediterranean mountain ranges diverged early, lineages occurring in northern lowland steppes are much younger (ca. 0.2 to 0.3 Ma), emphasizing the importance of southern European mountain ranges as long-term refugia. Recurrent colonization of the western Mediterranean region by eastern Mediterranean lineages and secondary contacts of currently spatially isolated lineages have significantly (co-)shaped the genetic structure within the group; we assume that these events may be a consequence of cold-stage range expansions. Based on combined genetic and morphometric data, we suggest treating the ten lineages introduced in this study as independent species, contrasting previous taxonomic treatments.

1. Introduction

The Eurasian steppes are among the largest biomes on Earth. Bordered by boreal forests to the North and (semi-)deserts to the South, macroclimate-driven (= zonal) steppes extend from the Pontic Plains in the Black Sea basin eastwards to Mongolia and China (Wesche et al., 2016). Outside the continuous distribution of zonal steppes, steppic grasslands also occur within mildly continental, predominantly forested areas if additional edaphic and microclimate-related factors enhance drought. Such plant communities are termed extrazonal or edaphic steppes; they usually occur on south-exposed, well-drained slopes or over sandy or gravelly soils (Ellenberg and Leuschner, 2010; Jännicke, 1892; Wesche et al., 2016). Highly disjunct islands of extrazonal steppes and similar xeric grasslands (Jäger, 1971; Loidi, 2017) are distributed throughout Europe, from the Iberian Peninsula in the west to the Balkan Peninsula and the Carpathians in the east, encompassing the inner-Alpine dry valleys and Central European areas, such as the Pannonian Basin or parts of the Kyffhäuser region in Germany (Braun-Blanquet, 1961; Braun-Blanquet and de Bolòs, 1957; Feurdean et al., 2018; Kajtoch et al., 2016; Magnes et al., 2021). The Carpathians and Balkan Mountains (Stara Planina) form a natural barrier to the adjacent zonal steppes in the east. The occurrence of numerous species in both zonal and extrazonal steppes reflects the ecological similarity of these habitats (e.g., *Astragalus onobrychis* L., *Cricetus cricetus* L., *Euphorbia seguieriana*

* Corresponding authors at: Department of Botany, University of Innsbruck, Sternwartestraße 15, 6020 Innsbruck, Austria.
E-mail addresses: Peter.Schonswetter@uibk.ac.at (P. Schönswetter), pau.carnicero@gmail.com (P. Carnicero).

https://doi.org/10.1016/j.ympev.2024.108242
Received 13 February 2024; Received in revised form 28 October 2024; Accepted 12 November 2024
Available online 16 November 2024

Neck., *Omocestus petraeus* Brisout de Barneville, *Stipa capillata* L.; Feoktistova et al., 2017; Frajman et al., 2019; Kirschner et al., 2020; Meusel et al., 1965; Záveská et al., 2019).

The Eurasian steppe biome has undergone massive climate-driven contractions and expansions. During cold stages of the Pleistocene, such as the Last Glacial Period (115 to 12 kya), the zonal Eurasian steppes had a much larger extent as compared to interglacial periods and repeatedly expanded into large parts of presently forested temperate Europe (reviewed in Hurka et al., 2019). During warm stages, forest expansion recurrently forced Eurasian steppe biota into disjunct and small interglacial refugia, i.e. today's extrazonal steppes (Stewart et al., 2010). Therefore, extrazonal steppes and their biota have traditionally been considered remnants of a continuous cold-stage steppe belt, which became isolated from each other and from the zonal steppes due to postglacial forest expansion at the onset of the Holocene, 11,700 years ago (Binney et al., 2017; De Soo, 1929; Jännicke, 1892). However, the divergence between zonal and extrazonal lineages of steppe biota may in fact be much older; vicariant separation in several typical steppe taxa occurred as early as the Mid-Pleistocene, ca. 1.4 Ma (Kirschner et al., 2023, 2022, 2020; Záveská et al., 2019). Warm-stage refugia of extrazonal steppes were often situated in mountainous areas, i. e. along the margin of the Pannonian Basin or in the Western Balkan Peninsula; such topographically diverse areas have likely provided suitable microclimates during varying climatic conditions (Athanassiou, 2012; Kryštufek et al., 2009; Pross et al., 2015), enabling the survival of biota during cold as well as warm periods (Egorov et al., 2020; Magyari et al., 2010, 2008; Varga, 2010; Willner et al., 2021).

Astragalus L. (milkvetch) is the most species-rich genus of xeric habitats in Eurasia. Within this genus, *Astragalus* sect. *Caprini* DC. is morphologically characterized by basifixed hairs, thickly textured legumes and relatively large yellow flowers arranged in typically few-flowered and short-stalked inflorescences (Podlech, 1999, 1988; Podlech and Zarre, 2013). It comprises ca. 300 diploid species (Podlech, 1988, 1986; Martin et al., 2008; Sytin 2009), that inhabit arid habitats ranging from lowlands up to the subalpine and alpine belt; their distribution extends from Northwestern Africa and Western Europe to Central Asia. In Northern Africa and Europe, *A.* sect. *Caprini* is represented by – depending on the taxonomic treatment – approximately a dozen taxa, which are morphologically differentiated based on characters related to floral and legume traits, hairiness of petals and leaflets, or length of the peduncle (Podlech, 1988; Podlech and Zarre, 2013). However, character states overlap, leading to different taxonomic treatments in the more widespread taxa (Supplementary Table S1). The mountain-dwelling taxa are generally narrowly distributed and rare, particularly in the Western Mediterranean, where all northwestern African and European members of *Astragalus* sect. *Caprini* (in the following abbreviated as AEMAC) are of high conservation interest. Critically endangered *A. cavanillesii* Podlech and *A. tremolsianus* Pau occur in the southeastern Iberian Peninsula (Lorite et al., 2007; Teso et al., 2018), and *A. maurus* (Humbert & Maire) Pau is limited to a few populations (< 5) in northern Morocco (Fougrach et al., 2007; Podlech and Zarre, 2013). In the Eastern Mediterranean, *A. hellenicus* Boiss. is a narrow endemic found only in southern Greece and rare, disjunctly distributed *A. nummularius* Lam. occurs in Crete, Lebanon and Syria (Podlech and Zarre, 2013; Strid and Tan, 1997).

In Europe, the two most widespread species of *A.* sect. *Caprini*, *A. dasyanthus* Pall. and *A. exscapus* L., are exclusively occurring in lowland steppes. The former is morphologically aberrant due to its caulescent habit and is the only species that occurs in sympatry with other members of this group. It is widespread from the southeastern Pannonian Basin and the Carpathian Basin through the zonal Eurasian steppes eastwards to western Kazakhstan (Podlech and Zarre, 2013). The latter is morphologically polymorphic and taxonomically controversial; for instance, above-mentioned *A. hellenicus* was included in *A. exscapus* subsp. *exscapus* by Podlech and Zarre (2013). *Astragalus exscapus* occurs in insular steppe habitats from the northeastern Iberian Peninsula over the inner-Alpine valleys, the Apennines and dry areas of Central Europe to the southern Balkan Peninsula and the northwestern Black Sea coast (Becker, 2010; Cancellieri et al., 2017; Ferrández Palacio, 2003; Goncharov et al., 1946; Meusel et al., 1965; Podlech and Zarre, 2013; Strid and Tan, 1997; Talavera and Castroviejo, 1999; Tutin et al., 1968). Two intraspecific entities, currently considered subspecies, are *A. exscapus* subsp. *transsilvanicus* (Schur) Nyár restricted to the Carpathian Basin (Ciocârlan, 2000; Podlech and Zarre, 2013; Szabo et al., 2021) and more widespread *A. exscapus* subsp. *pubiflorus* (DC.) Soó. However, their ranges and delimitation are contradictory in national floras and taxonomic treatments (Supplementary Table S1). *Astragalus exscapus* subsp. *pubiflorus* is scattered in the mountains of Albania, Bulgaria and northwestern Greece while it is more abundant in steppic grasslands of the Pontic Plains (Assyov et al., 2012; Barina, 2017; Chifu et al., 2006; Ciocârlan, 2000; Mosyakin and Fedoronchuk, 1999; Petrova and Vladimirov, 2009; Pils, 2016; Podlech, 1988; Podlech and Zarre, 2013; Qosja et al., 1992; Strid and Tan, 1997; Tutin et al., 1968).

The zonal Eurasian steppes are one of the most threatened biomes worldwide mostly due to agricultural intensification; the same applies to the westerly adjacent extrazonal steppes of the Pannonian Plains (Cremene et al., 2005; Dengler et al., 2014; Kamp et al., 2016; Parnikoza and Vasiluk, 2011; Török et al., 2018). Among the different types of xeric grasslands, steppes with fairly deep topsoil – which are typical habitats for species of *A.* sect. *Caprini* – are especially susceptible to negative developments (Mucina et al., 1993), conferring a high regional extinction risk for the constituent species. The situation of extrazonal steppes – at least of those in low elevations – is similarly dramatic. For instance, populations of widespread *A. exscapus* L. are in strong decline throughout its distribution area; at least 44 % of all known German populations have become eradicated in the last 150 years (Becker, 2010, 2003), only a single individual-rich population is left in Austria (Schratt-Ehrendorfer et al., 2022), and less than 150 individuals remain in two recently discovered localities in northern Serbia (Diklić, 1972; Stevanović et al., 1999; N. Kuzmanovic, University of Belgrade, pers. comm.). The main threats include land use changes such as abandonment of pasturing and mowing and the influx of nitrogen and urbanization (Dengler et al., 2020; Molnár et al., 2012; Török et al., 2018; Willner et al., 2021). Accordingly, most of the lowland steppe species and some of the mountain-dwelling species of *A.* sect. *Caprini* are in the focus of conservation efforts, for instance *A. cavanillesii*, *A. dasyanthus*, *A. exscapus* subsp. *exscapus, A. exscapus* subsp. *pubiflorus, A. exscapus* subsp. *transsilvanicus*, and *A. tremolsianus* (Bondarchuk and Rakhmetov, 2018; Ciocârlan, 2013; Iriondo et al., 2009; Kienberg and Becker, 2017; Kukula et al., 2003; Lorite et al., 2007; Teso et al., 2018).

Taken together, AEMAC are not only disjunctly distributed, rare and threatened, but also morphologically highly similar, resulting in incongruences across taxonomic treatments (Podlech, 1988; Podlech and Zarre, 2013; Tutin et al., 1968; Supplementary Table S1). Previous phylogenetic studies have consistently shown that *A.* sect. *Caprini* forms an early-diverging, monophyletic clade within *Astragalus* (Azani et al., 2019, 2017; Kazemi et al., 2009; Kazempour Osaloo et al., 2005, 2003; Su et al., 2021). However, they failed to corroborate species circumscriptions and to estimate relationships among species due to the lack of resolution of the employed genetic markers (ETS, and three plastid regions: Riahi et al., 2011; ITS: Sheikhakbari-Mehr and Maassoumi, 2017), likely due to the group's recent diversification. Consequently, molecular approaches based on a high number of single nucleotide polymorphisms (SNPs) are likely more suitable for reconstructing relationships among the closely related taxa. Finally, apart from the scientifically-motivated striving for sound phylogenetic hypotheses in under-investigated plant groups, taxonomic concepts such as wide or narrow circumscription of species directly bear on nature conservation, for instance the range-wide threat category.

Here, we used SNP data derived from restriction-site associated DNA sequencing (RADseq), nuclear ribosomal internal transcribed spacer (ITS) sequences, maternally inherited (for Fabaceae: Corriveau and Coleman 1988) plastid DNA sequences and morphometric data

alongside relative genome size (RGS) to elucidate the group's spatio-temporal diversification. (1) The first goal was to unravel whether the populations of (sub-)mediterranean mountain systems from the Iberian and Balkan peninsulas originated early in the group's diversification, whereas populations from lowland steppes originated later. This would reflect the long-term climatic stability of the (sub-)mediterranean mountain areas in contrast to the recurrent and large-scale range alterations of lowland steppes as a response to the climatic oscillations of the Pleistocene. (2) The second goal was to evaluate whether the disjunct distribution exhibited by AEMAC results from vicariance due to fragmentation of their continuous cold-stage habitats during warm stages of the Pleistocene or rather from long-distance dispersals. We further discuss to what extent the recurrent climatic cycles of the Pleistocene have fueled speciation, lineage formation and secondary contacts within AEMAC. (3) Finally, we aimed to clarify the group's taxonomy based on an integrative approach combining genomic and genetic evidence as well as RGS and morphometric data. Amongst other, we reevaluate the circumscription of *A. exscapus*, a flagship species of dry grassland conservation in Europe (Becker, 2013).

2. Material and methods

2.1. Study species

To increase readability, from here onwards taxonomy and nomenclature deviate from the treatment by Podlech and Zarre (2013) in anticipation of our results. Specifically, we use the species rank for all AEMAC taxa, including *A. exscapus* subsp. *transsilvanicus* and *A. exscapus* subsp. *pubiflorus*. The latter is split into the two informal units, "A. pubiflorus Pontic" and "A. pubiflorus Balkan". Further, the populations from southern Greece are treated as *A. hellenicus* and not as *A. exscapus* subsp. *exscapus*, following Flora Hellenica (Strid and Tan, 1997). Finally, we treat population 6 from northeastern Spain as *A. cavanillesii* and not *A. exscapus*, as originally published (Ferrández Palacio, 2003).

We included *A. maurus* from Morocco as well as all AEMAC taxa distributed north of the Mediterranean Sea from the Iberian Peninsula in the West to the western Pontic Plains in the East in the RADseq dataset except for *A. caprinus* L. subsp. *huetii* Bunge (Sicily) and *A. ictericus* Dingler (northern Greece; Supplementary Table S2). *Astragalus aegobromus* Boiss. and Hohen. (33), *A. angustiflorus* subsp. *angustiflorus* K. Koch (31) and *A. flexus* Fisch. (34), distributed across the Irano-Turanian region were added as outgroups based on phylogenetic evidence (Azani et al., 2019, 2017; Riahi et al., 2011; Su et al., 2021) and overall morphological similarity (Podlech, 1988; Podlech and Zarre, 2013). For the plastid DNA data set, the outgroup sampling was extended by adding 21 newly generated sequences of 19 taxa (Supplementary Table S2). Additionally, *ycf1* sequences of the following species were downloaded from GenBank and included in the alignment: *A. americanus* (Hook.) M. E. Jones MZ923737, *A. annularis* Forssk. MK958285, *A. frigidus* (L.) A. Gray JQ801559, *A. membranaceus* (Fisch.) Bunge var. *membranaceus* KX255662, *A. mongholicus* Bunge MT982389, *A. remotijugus* Boiss. and Hohen. MK958287, *A. vulpinus* Willd ON550388. The ITS alignment was complemented by six newly generated sequences of five taxa (Supplementary Table S2) and by sequences from GenBank of *A. alopecurus* Pall. MF543748, *A. annularis* KX954894, *A. caprinus* subsp. *caprinus* KX954920, *A. frigidus* AB231092, *A. membranaceus* HQ891827, *A. mongholicus* MN224267, *A. ponticus* Pall. AB741296, *A. sieversianus* Pall. MK945637, *A. vulcanicus* Bornm. AB051960 and *A. vulpinus* MT923555.

2.2. Plant material

Leaf material (one to three leaflets per individual) of 32 populations (AEMAC: 21, outgroup: 11) was collected in silica gel between 2011 and 2022. Collecting permits are cited in Supplementary Table S2. For AEMAC, usually five individuals per population were sampled, totalling 88 individuals, whereas for the outgroup species one to two individuals per population were collected, totalling 17 individuals (Supplementary Table S2). We identified the plants using different Floras (Chamberlain and Matthews, 1969; Tutin et al., 1968; Fischer et al., 2008; Goncharov et al., 1946; Podlech and Zarre, 2013; Strid and Tan, 1997). Additionally, herbarium material from the herbaria BC, B, IB, M, MSB, MA, and W (Holmgren, 1990) was sampled for plastid sequencing, totalling 16 individuals (7 AEMAC, 9 outgroup populations; Supplementary Table S2). A recently collected herbarium voucher of *A. maurus* (BA 967836, Supplementary Table S2) was used to complement the RADseq dataset, totalling 89 individuals from 22 AEMAC populations. Except for widespread *A. dasyanthus*, the sampling localities cover well the distribution range of the species. For the morphometric measurements, herbarium specimens covering the distribution areas of all investigated taxa were made available by the herbaria B, G, M, MSB, MA, and IB (Supplementary Table S3).

2.3. DNA extraction, amplification, sequencing and analyses of the plastid marker *ycf1*

Extraction of total genomic DNA from silica-dried leaf material and herbarium specimens followed the CTAB protocol used by Frajman and Schönswetter (2011). Mapping RAD loci against the reference plastid genome (Laczkó et al., 2022) of *A. flexus* ON550403 yielded no sufficient information within AEMAC (7 *PstI* cut sites, ca. 1300 bp, two variable sites, data not shown). Therefore, we decided to use the highly variable plastid region *ycf1* (Bartha et al., 2012). Amplifications and sequencing were done as described by Záveská et al. (2019). Typically, two individuals per population were sequenced, with the exception of populations 1, 2, 15, 16 and 28 from which a single individual was sequenced. As no intrapopulational variation was found, only one individual per population was used for the subsequent analyses. Sequences were aligned using MAFFT (https://mafft.cbrc.jp/alignment/server/) and the alignment was improved manually in BioEdit 7.0.0. (Hall, 1999). In all analyses, indels were treated as missing values.

A haplotype network based on an 883 bp alignment including all 26 sequenced AEMAC individuals plus one representative each of closely related *A. angustiflorus* subsp. *angustiflorus* and *A. angustiflorus* subsp. *anatolicus* (Boiss.) D.F.Chamb. was constructed using statistical parsimony as implemented in TCS 1.21 (Clement et al., 2000) with PopART (Leigh and Bryant, 2015). Analyses were run with the default parsimony connection limit of 95 %.

We used BEAST 2.7.5 (Bouckaert et al., 2019) for reconstruction of relationships and estimation of divergence times. As there are no reliable fossils (Wojciechowski, 2005) that can be assigned unambiguously to *Astragalus* or other closely related taxa in the IR-Lacking Clade of Faboideae (IRLC; Lavin et al., 2005; Wojciechowski et al., 1999), the *ycf1* data was secondarily calibrated on three nodes with the inferred ages from Su et al. (2021, calibration node 1 and 2) and Azani et al. (2019, calibration node 3): (1) the crown age of *Astragalus* (mean: 12.51 Ma, *SD*: 1.6), (2) the crown age of the "Phaca clade" *sensu* Su et al. 2021 (mean: 7.20 Ma, *SD*: 0.85), and (3) the crown age of *A.* sect. *Caprini* (mean: 2.33 Ma, *SD*: 0.6). The *ycf1* alignment was 1,051 bp long. After model testing with ModelFinder (Kalyaanamoorthy et al., 2017), the TPM3uf + G4 substitution model was chosen based on the Bayesian information criterion (BIC). Further, a relaxed clock model with a Birth-Death prior (Heled and Drummond, 2015) was selected. Two independent analyses were run for 100 million generations each, sampling every 10,000 generations. To assess convergence and ensure that the effective sample size (ESS) for all parameters was > 200, log files were analyzed using Tracer 1.7.2 (Rambaut et al., 2018). Resulting trees of both analyses were combined using LogCombiner 2.7.5, omitting the first 20 % of trees as burn-in. A maximum clade credibility (MCC) tree based on 16,000 trees and showing median heights was built using TreeAnnotator 2.7.5 and visualized using FigTree 1.4.4 (Rambaut, 2016).

2.4. Amplification, sequencing and analyses of the internal transcribed spacer (ITS)

The amplification of the ITS region was done in 20 µl reactions using 8 µl REDTaq PCR Reaction Mix (Sigma-Aldrich), 0.9 µl BSA (1 mg/ml; Promega), 0.55 µl (10 µM) of both primers (17SE and 26SE, Sun et al., 1994) and 1 µl of 1:10 diluted DNA of unknown concentration. To enhance the specificity of the primer pair, we used a touchdown PCR program of 35 cycles with 30 s at 94 °C, starting annealing temperature of 56 °C, which was decreased by 0.4 °C each cycle until 48° C from where on it stayed constant, 1 min at 72 °C. The final extension step was 72 °C for 10 min. Control for amplification success, enzymatic purification and sequencing was done as described for *ycf1*. After identical sequences were removed from the final alignment, a total of 19 ribotypes were retained. ModelFinder (Kalyaanamoorthy et al., 2017) was used to select the appropriate substitution model. Based on the BIC, K80 was chosen and AEMAC was constrained as monophyletic. The dataset was secondarily calibrated with a normal prior using the same calibration nodes, settings and downstream analyses as described above for the plastid dataset.

2.5. RADseq: Library preparation, identification of RADseq loci and SNP calling

The final RADseq dataset included 22 AEMAC populations (totalling 89 individuals, mean: 4.05 individuals per population) and 3 populations from the outgroup totalling 7 individuals. Single-digest RADseq libraries were prepared from one to five individuals per population using the restriction enzyme PstI (New England Biolabs) and a protocol adapted from Paun et al. (2016) employing a double barcoding approach. Four individuals were sequenced twice to assess the reproducibility of the method. A 6-base-pair (bp) P2 barcode and a 14-bp P1 barcode that differed by at least three bases from each other were selected to avoid erroneous assignment of fragments due to sequencing errors. We started with 140 ng DNA per individual and ligated 0.2 µM P1 adapters to the restricted samples. Shearing by sonication was performed with a M220 Focused-ultrasonicator (Covaris) with settings targeting a size range of 200–800 bp and a mode at 400 bp (peak in power: 50, duty factor 10 %, 200 cycles per burst and treatment time 90 s at 20 °C). To remove undesired fragment lengths from each pool, left- and right-side size selection steps were done, using × 0.7 and × 0.55 vol of SPRIselect reagent (Beckman Coulter). After ligation of P2 adaptors, DNA content of each sample was quantified using a Qubit 4 Fluorometer (Thermo Fisher Scientific), and samples were pooled to be equally represented in the final sample. Further, size selection steps were done on the left side with × 0.55 vol of SPRI reagent before and after the 18 cycles of PCR amplification with Phusion Master Mix (Thermo Fisher Scientific). The libraries were sequenced on a NovaSeq SP SR100 XP and a HiSeq2000 sequencer (Illumina) at CSF Vienna (https://csf.ac.at/facilities/next-generation-sequencing/) as 100-bp single reads.

Raw reads were quality filtered and demultiplexed based on individual-specific barcodes using Picard BamIndexDecoder included in the Picard Illumina2bam package (available from https://github.com/wtsinpg/illumina2bam) and the program process_radtags.pl implemented in Stacks 2.3 (Catchen et al., 2013, 2011). The RADseq loci were further assembled, and SNPs were called using the denovo_map.pl pipeline also implemented in Stacks. Based on the optimization process described by Paris et al. (2017), the parameters which yielded most polymorphic loci were chosen for subsequent analyses. Minimum coverage to identify a stack in denovo_map.pl (Catchen et al., 2013, 2011) was set to 3 (-m 3), the maximum number of differences between two stacks in a locus in each sample was three (-M 3), and the maximum number of differences among loci to be considered as orthologous across multiple samples was three (-n 3). The program populations implemented in Stacks 2.3 was used to pre-process and export the selected loci using different filtering settings according to the requirements of each respective analysis (Table 1; Catchen et al., 2013, 2011). For all analyses, a maximum heterozygosity filter (–max_obs_het 0.65) was used to filter potential paralogs.

2.6. Phylogenetic and dating analyses based on SNP data

A maximum likelihood (ML) phylogeny was computed using RAxML 8.2.8 (Stamatakis, 2014) to infer phylogenetic relationships. SNP data was pre-processed and exported to VCF format using populations (settings in Table 1; Catchen et al., 2013, 2011). Indels were removed and SNPs with a minimum coverage lower than ten were filtered using VCFtools (–minDP 10; Danecek et al., 2011). The VCF-file was then converted to Phylip format with the vcf2phylip script (Ortiz, 2019). Invariant sites were removed from the original Phylip file using the –E flag in RAxML (Stamatakis, 2014), resulting in 23,387 variant SNPs, and Felsenstein's ascertainment bias correction was used to account for missing invariant sites (Leaché et al. 2015). Tree searches were done under a General Time Reversible model with categorical optimization of substitution rates (ASC_GTRCAT), using the –K80 flag to assign a Kimura 80 (Kimura, 1980) substitution model (Stamatakis, 2014). The best-scoring ML tree was bootstrapped using 150 replicates and the frequency-based stopping criterion (Pattengale et al., 2010).

As the more recent splits were not fully resolved by the plastid and ITS phylogenies, we estimated divergence times using RADseq data with SNAPP (Bryant et al., 2012), a package implemented in BEAST 2 (Bouckaert et al., 2019). Due to the computational demand of SNAPP a reduced dataset containing one to two samples per species was used; individuals with the lowest amount of missing SNPs per individual were selected. Populations 16 and 17 of "A. pubiflorus Pontic" were excluded due to high missing data. The input file was prepared using the script snapp_prep.rb (available at https://github.com/mmatschiner/snapp_prep) and consisted of 9,708 bi-allelic unlinked sites and 16

Table 1
Final number of individuals (N Inds) and number of SNPs (N SNPs) available for each analysis after specific data pre-processing and filtering. Settings used for SNP export in populations (Catchen et al., 2013, 2011) are provided for each respective analysis; –R (minimum percentage of individuals across populations required to process a locus), –min-maf (minimum minor allele frequency required to process a SNP and corresponding number of individuals), –max-obs-het (maximum observed heterozygosity required to process a SNP), –write-single-SNP (restrict data analysis to only the first SNP per locus).

Analysis	–R	--min-maf	--max-obs-het	--write-single-SNP	N Inds	N SNPs
Dsuite (Malinsky et al., 2021)	0.5	0.0105 (=1 ind)	0.65	not used	91	251,375
RAxML (Stamatakis, 2014)	0.9	0.0315 (=3 inds)	0.65	not used	95	23,387
SNAPP (Bryant et al., 2012)	1	–	0.65	used	16	9,708
Splitstree (Huson and Bryant, 2005)	0.5	0.0112 (=1 ind)	0.65	not used	89	223,419
Structure (Pritchard et al., 2002)	0.5	0.0112 (=1 ind)	0.65	used	89	51,873

individuals (for details see Table 1). We used secondary calibration points obtained from dating analysis of the plastid dataset (described above), applying a lognormal prior (crown age *A. angustiflorus* subsp. *anatolicus* plus AEMAC: mean: 0.72, *SD*: 0.2; onset of diversification of AEMAC: mean: 0.57, *SD*: 0.2). A Gamma distribution was assigned to the Lambda prior, with an Alpha of 1 and a Beta of 200, and the mutation rate was estimated. Three independent iterations were run, each with a chain length of 2,000,000, sampled every 100 generations. This resulted in 60,000 trees. Effective sample size (ESS) for all parameters in each run was > 200, log files were analyzed using Tracer 1.7.2 (Rambaut et al., 2018). After removing 20 % of trees from each run as burn-in, we combined the remaining 48,000 trees with LogCombiner 2.7.5, summarized the MCC tree with median heights in Treeannotator 2.7.5, and visualized the final tree using FigTree 1.4.4 (Rambaut, 2016).

For the 89 AEMAC individuals, SplitsTree 4.12.6 (Huson and Bryant, 2005) was used to create a NeighborNet to visualize potential reticulations. The analysis was based on a dataset with relatively relaxed filtering settings (Table 1). Network analysis was done using the NeighborNet method based on Nei's standard genetic distances between individuals (Nei, 1972), which were calculated from the individual genotype calls using the R package StAMPP 1.5.1 (Pembleton et al., 2013).

2.7. Ancestral range estimation

To infer the biogeographical history of AEMAC from the phylogenies produced with RAxML and SNAPP, we used the R package BioGeoBEARS 1.1.3 (https://github.com/nmatzke/BioGeoBEARS; Matzke, 2013, 2014) for R 4.4.0 (https://www.R-project.org/). The RAxML tree was made ultrametric using the Software Mesquite 3.81 (https://www.mesquiteproject.org; Maddison and Maddison, 2023). The populations were assigned to the following ecoregions based on their occurrence. (A) Western Irano-Turanian Region, (B) Eastern Mediterranean mountain steppes, (C) Western Mediterranean mountain steppes, (D) Western lowland steppes, (E) Eastern lowland steppes. As a migration hypothesis we assumed that migration within and between regions is free (manual_dispersal_multipliers was set to 1) and the maximum range size was set to 3. Two models were tested (DEC, DIVALIKE), each with and without the parameter *j* which allows for founder-event speciation ("rare jump dispersal event").

2.8. Exploring gene flow using ABBA-BABA tests, f-branch statistics and Bayesian clustering

Patterson's *D* statistic (ABBA-BABA; Green et al., 2010; Martin et al., 2015; Patterson et al., 2012) was used to explore potential gene flow between the six main RADseq clades (see Results). *D* statistics and the related admixture fraction estimates (*f4*-ratio statistics) were calculated using the software Dsuite (Malinsky et al., 2021). Input data was filtered and pre-processed as shown in Table 1. Dsuite uses a jackknifing approach to assess correlations in allele frequencies between closely related lineages. Tests were designed with a fixed phylogeny of three ingroup populations and one outgroup population (((P1,P2)P3)O), wherein a typical ancestral ("A") and derived ("B") allele pattern should follow BBAA. Under incomplete lineage sorting, conflicting ABBA and BABA patterns are expected to occur in equal frequencies, resulting in the *D* statistic equalling zero. If, however, introgression occurred between P3 and P1 or P2, one would expect an excess of shared alleles and the *D* statistic should therefore be significantly different from zero (Durand et al. 2011). The *f*-branch or f_b(C) metric, a summary of *f4* admixture ratios showing excess allele sharing between the branch on the y-axis and the sample on the x-axis was used to tease apart potentially correlated *f4*-ratio statistics and estimate gene flow between internal branches of the RAxML phylogeny (P1-P3; Malinsky et al., 2021). Within Dsuite, the Dtrios and Fbranch flags were used to identify introgression between all combinations of the six RADseq groups, specifying *A. angustiflorus* subsp. *angustiflorus* as the outgroup and applying Bonferroni correction to account for the increased risk of a type I error when making multiple statistical tests. A separate and subsequent, in-depth analysis was done for the western Mediterranean species and *A. nummularius*, using *A. angustiflorus* subsp. *angustiflorus* as the outgroup (24 individuals in total). The test was done using the two conflicting tree topologies inferred by RAxML and SNAPP. The input data was generated using the same settings as in case of the full dataset (Table 1), whereas this specific dataset contained 90,880 SNPs after preprocessing. We considered a gene flow signal as significant if the following combination of parameters were fulfilled in a test: $D \neq 0$, $Z > 3$ and p-value < 0.05 (Durand et al., 2011; Ottenburghs et al., 2017).

Bayesian clustering as implemented in Structure 2.3.4 (Falush et al., 2003; Pritchard et al., 2000a) was used to estimate the number of demes and to determine the degree of admixture. For this, a SNP dataset without outgroups was generated using populations (settings in Table 1; Catchen et al., 2013, 2011, 2011). Clustering was done using the Admixture model (Alexander et al., 2009), for $K = 1$–10 clusters and ten replicates per *K*. Each replicate was run with 100,000 MCMC iterations after an initial burn-in of 50,000 iterations. The best *K* was determined following Evanno et al. (2005) using Structure Harvester (Earl and vonHoldt, 2012). The output of Structure Harvester was further processed with CLUMPP (Jakobsson and Rosenberg, 2007) to align cluster assignment across replicates.

2.9. Relative genome size measurements

Relative genome size (RGS) was inferred from fluorescence intensities of 4′,6-diamidino-2-phenylindole (DAPI)-stained nuclei isolated from silica-gel dried leaf material following Suda and Trávníček (2006). *Bellis perennis* L. served as the internal reference standard (2C = 3.38 pg DNA; Schönswetter et al., 2007) for all samples. One to five individuals each from 21 AEMAC populations were analysed (average 4.28; in total 83) and two individuals were measured from each of the three outgroup populations (Supplementary Table S2). For populations 1 and 2 of *A. maurus*, 4 and 5 of *A. cavanillesii*, and 28 of *A. nummularius*, RGS could not be determined as the plant material was of insufficient quality or not suitable for flow cytometry (i.e. provided as DNA extract in the case of *A. nummularius*). Desiccated green leaf tissue (~ 0.5 cm^2) was chopped together with an appropriate amount of fresh reference standard and processed as described in Doležel et al. (2007). The relative fluorescence intensity of 3,000 particles was recorded with a Partec CyFlow space flow cytometer (Partec). Partec FloMax software (Partec) was used to evaluate the histograms. The reliability of the measurements was assessed by calculating coefficients of variation (CVs) for the G1 peaks of both the analyzed sample and the reference standard. Histograms resulting from analyses yielding a CV threshold of > 5 % were manually gated. Boxplots were created in R 4.1.2 (R Core Team, 2021) and a map showing the mean RGS of each investigated population was constructed in QGIS 3.22 (https://qgis.osgeo.org).

2.10. Morphometric analyses

Morphological differentiation was investigated across 137 individuals from 85 AEMAC populations (Supplementary Table S3). From each of the investigated species, material of at least three individuals was available for the morphometric measurements: *A. cavanillesii* (n = 14), *A. dasyanthus* (n = 31), *A. exscapus* (n = 36), *A. hellenicus* (n = 16), *A. maurus* (n = 3), *A. nummularius* (n = 15), "A. pubiflorus Pontic" (n = 6), "A. pubiflorus Balkan" (n = 3), *A. transsilvanicus* (n = 10), *A. tremolsianus* (n = 3). Based on descriptions in the literature and a preliminary screening, eleven morphological characters were measured with a caliper on the herbarium vouchers: calyx teeth length in mm (1), maximal width of calyx tube in mm (2), leaf length in mm (3), length of a middle leaflet in mm (4), number of leaflets per leaf (excl. terminal leaflet) (5), width of a middle leaflet in mm (6), pedicel length in mm (7), peduncle length in mm (8), petiolule length in mm (9), standard

length in mm (10), and stipule length in mm (11). Further, the number of hairs on the entire abaxial surface of the standard was determined (12, also shown as binary character [absent/present] in Fig. 7). Finally, a ratio (13) was calculated from characters 4 and 7, resulting in a final matrix of thirteen characters. Each value typically represents the mean of three measurements. Generative and vegetative characters were scored on fully developed organs. Correlation among measured characters was tested by Pearson and Spearman correlation coefficients, depending on the distribution of values. Principal component analysis (PCA) of standardized variables was conducted with the function

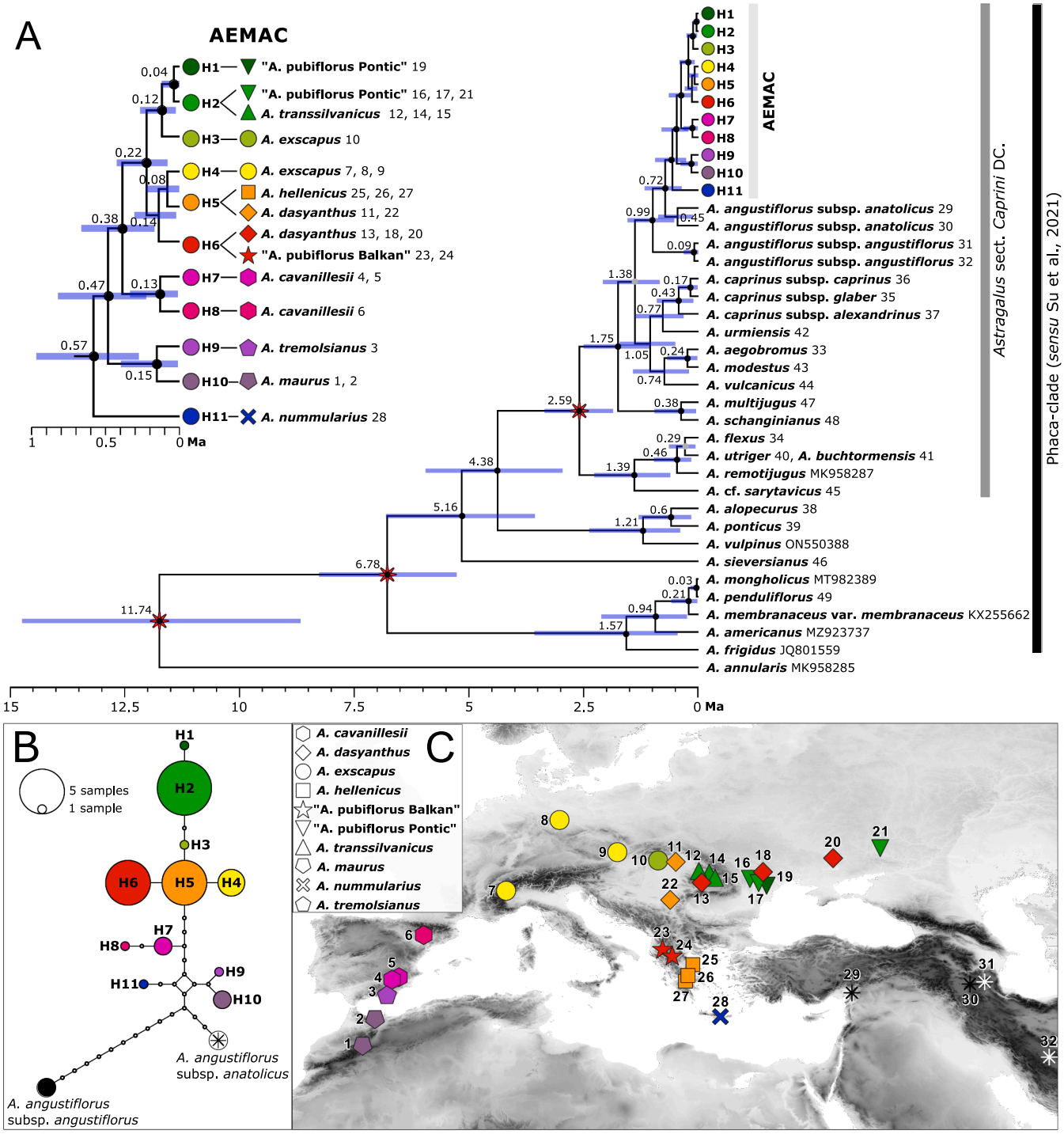

Fig. 1. Temporal diversification and spatial variation of the plastid *ycf1* region among northwestern African and European members of *Astragalus* sect. *Caprini* (AEMAC). Symbols indicate taxa, numbers in A and C are population identifiers (Supplementary Table S2), and colors correspond to haplotypes (labeled H1–H11 in B). A, time-calibrated maximum clade credibility tree including AEMAC and 26 outgroup taxa. Numbers above branches are median ages in million years ago (Ma). Black and gray circles indicate nodes with posterior probabilities (PP) ≥ 0.95 and PP 0.85–0.94, respectively. Red stars indicate secondary calibration points (see section 2.3 for details) and blue bars represent 95 % highest posterior densities intervals. B, statistical parsimony network showing relationships among haplotypes. Sizes of circles reflect haplotype frequencies. Unsampled haplotypes are shown as small uncolored circles. C, geographic distribution of the haplotypes and species. Black and white stars correspond to the outgroup *A. angustiflorus* subsp. *anatolicus* and *A. angustiflorus* subsp. *angustiflorus*, respectively. (For interpretation of the references to colour in this figure legend, the reader is referred to the web version of this article.)

prcomp and visualized with the R package ggplot2 using R 4.1.2 (R Core Team, 2021; Wickham et al., 2016) to demonstrate the overall variation pattern along the first two components. Two separate PCA ordinations were calculated. In the first dataset, all 137 individuals were included and twelve of the 13 characters were used (character 3 was excluded based on initial trials to improve resolution). For the second PCA 88 individuals were analyzed, after excluding the three morphologically most divergent species *A. dasyanthus*, *A. nummularius* and *A. tremolsianus*, and 10 characters were used; characters 2, 8 and 9 were excluded to improve resolution. The second PCA was done to enhance the morphological separation within the more similar taxa. Based on the morphometric data, we produced an identification key. Metric values presented there correspond to the 10th and 90th percentiles, supplemented by extreme values in parentheses.

3. Results

3.1. Phylogenetic relationships and divergence times based on plastid ycf1 sequences

The 38 *ycf1* sequences for the molecular dating approach were 817–901 bp long (GenBank accession numbers in Supplementary Table S2); the final alignment was 1,035 bp long and contained 359 variable and 274 parsimony-informative sites resulting in an overall nucleotide variability of 34.69 %. The AEMAC (populations 1–28) were resolved as monophyletic and diverged from their closest relative, *A. angustiflorus* subsp. *anatolicus* in the Mid-Pleistocene 0.72 Ma (95 % highest posterior densities, HPD: 0.36–1.17; Fig. 1A). The onset of the AEMAC diversification was dated to 0.57 Ma (95 % HPD: 0.27–0.94), leading to the origin of eastern Mediterranean *A. nummularius*; western Mediterranean *A. maurus* and *A. tremolsianus* diverged 0.47 Ma (95 % HPD: 0.22–0.8; Fig. 1A). Subsequently, western Mediterranean *A. cavanillesii* diverged 0.38 Ma (95 % HPD: 0.17–0.65; Fig. 1A). The major split between the other European lineages, including mountain and lowland steppe taxa, occurred 0.22 Ma (95 % HPD: 0.08–0.41; Fig. 1A); diversification within these two major clades took place between 0.14 Ma (95 % HPD: 0.02–0.3) and 0.04 Ma (95 % HPD: 0.0–0.12; Fig. 1A). The estimated mutation rate of *ycf1* was 0.0099 substitutions/site/Ma (95 % HPD: 0.0077–0.0121 substitutions/site/Ma).

The alignment used to infer a haplotype network, which included 28 AEMAC populations as well as the outgroups *A. angustiflorus* subsp. *angustiflorus* and *A. angustiflorus* subsp. *anatolicus* (populations 29, 31),

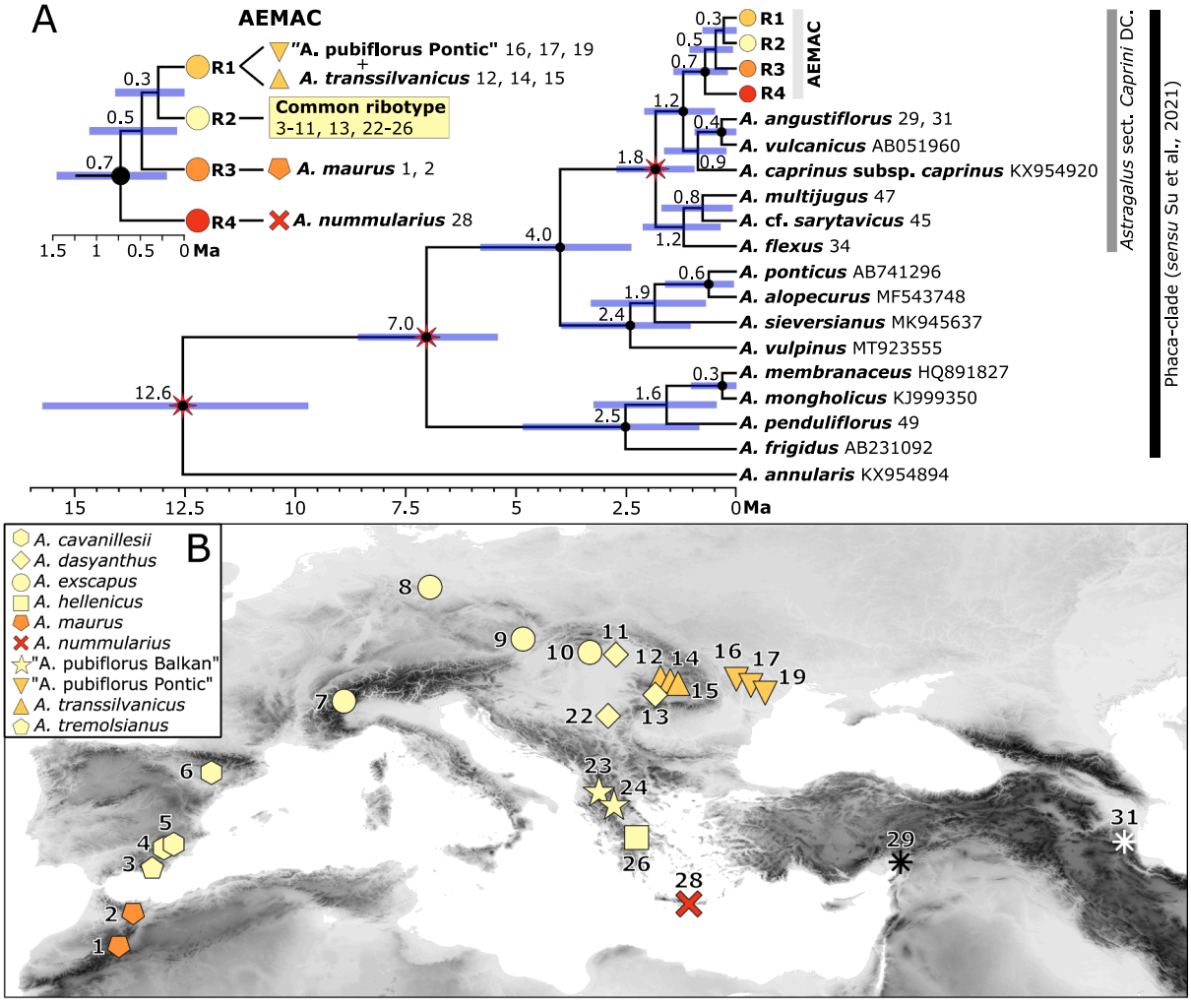

Fig. 2. Internal transcribed spacer (ITS) variation among northwestern African and European members of *Astragalus* sect. *Caprini* (AEMAC). Symbols indicate taxa, numbers in A and B are population identifiers (Supplementary Table S2), and colors correspond to ribotypes (labeled R1–R4). A, time-calibrated maximum clade credibility tree including AEMAC and 16 outgroup taxa. Numbers above branches are median ages in million years ago (Ma). Black dots indicate maximally supported nodes (posterior probability 1). Red stars indicate secondary calibration points and blue bars represent 95% highest posterior densities intervals. B, distribution of ribotypes. Symbols indicate taxa, numbers are population identifiers (Supplementary Table S2). The black and white star indicates the location of *A. angustiflorus* subsp. *anatolicus* (29) and *A. angustiflorus* subsp. *angustiflorus* (31), respectively. (For interpretation of the references to colour in this figure legend, the reader is referred to the web version of this article.)

contained 30 sequences ranging from 829–865 bp and was 883 bp long. The matrix comprised 33 variable nucleotide characters, 15 parsimony-informative sites and two indels (36 and 18 bp long), resulting in 3.73 % variable characters (indels not included). In total, 11 haplotypes (H) were revealed (Fig. 1BC). H1–H6 were separated by maximally five mutational steps. The closely related H1 and H2 were found in "A. pubiflorus Pontic" and *A. transsilvanicus*, whereas H3 and H4 were detected exclusively in *A. exscapus*. While *A. hellenicus* and *A. dasyanthus* shared H5, H6 was discovered in "A. pubiflorus Balkan" and *A. dasyanthus*. H7 and H8 were restricted to *A. cavanillesii* from southern and northern Iberian Peninsula, respectively. H9 corresponded to *A. tremolsianus* and the closely related H10 belonged to *A. maurus*. The earliest-diverging species within AEMAC, *A. nummularius,* possessed H11.

3.2. Phylogenetic relationships and divergence times based on ITS sequences

The ITS alignment was 606 bp long and harboured 85 variable and 26 parsimony-informative sites resulting in an overall nucleotide variability of 14.02 %. The 19 sequences which were included ranged from 601–603 bp (GenBank accession numbers in Supplementary Table S2). According to the dated ITS phylogeny (Fig. 2), AEMAC diverged in the Early Pleistocene 1.2 Ma from the ancestors of a clade comprising *A. angustiflorus, A. caprinus* subsp. *caprinus* and *A. vulcanicus* (95 % HPD: 0.50–2.1). Monophyletic AEMAC started to diversify in the Mid-Pleistocene 0.7 Ma (95 % HPD: 0.2–1.44), and comprised four ribotypes (R1–R4; Fig. 2). *Astragalus nummularius* was resolved as the earliest-diverging lineage, followed by *A. maurus* 0.5 Ma (95 % HPD: 0.09–1.07). Finally, the last split occurred 0.3 Ma (95 % HPD: 0.002–0.78) and resulted in a common and widespread ribotype shared by the larger part of populations on the one hand and a ribotype shared by only *A. transsilvanicus* and "A. pubiflorus Pontic" on the other hand. Generally, ITS sequence divergence was shallow, and the ribotypes of *A. maurus*, *A. nummularius* and "A. pubiflorus Pontic"/*A. transsilvanicus* deviated from the common ribotype by only one substitution. Ribotypes within AEMAC were separated by maximally two mutational steps (data not shown). Further, *A. aegobromus* and *A. urmiensis* Bunge had the same ribotype as *A. angustiflorus* and *A. caprinus* subsp. *caprinus*, respectively. Hence, the former two taxa were excluded (Fig. 2). The estimated mutation rate of ITS was 0.0031 substitutions/site/Ma (95 % HPD: 0.0022–0.0042 substitutions/site/Ma).

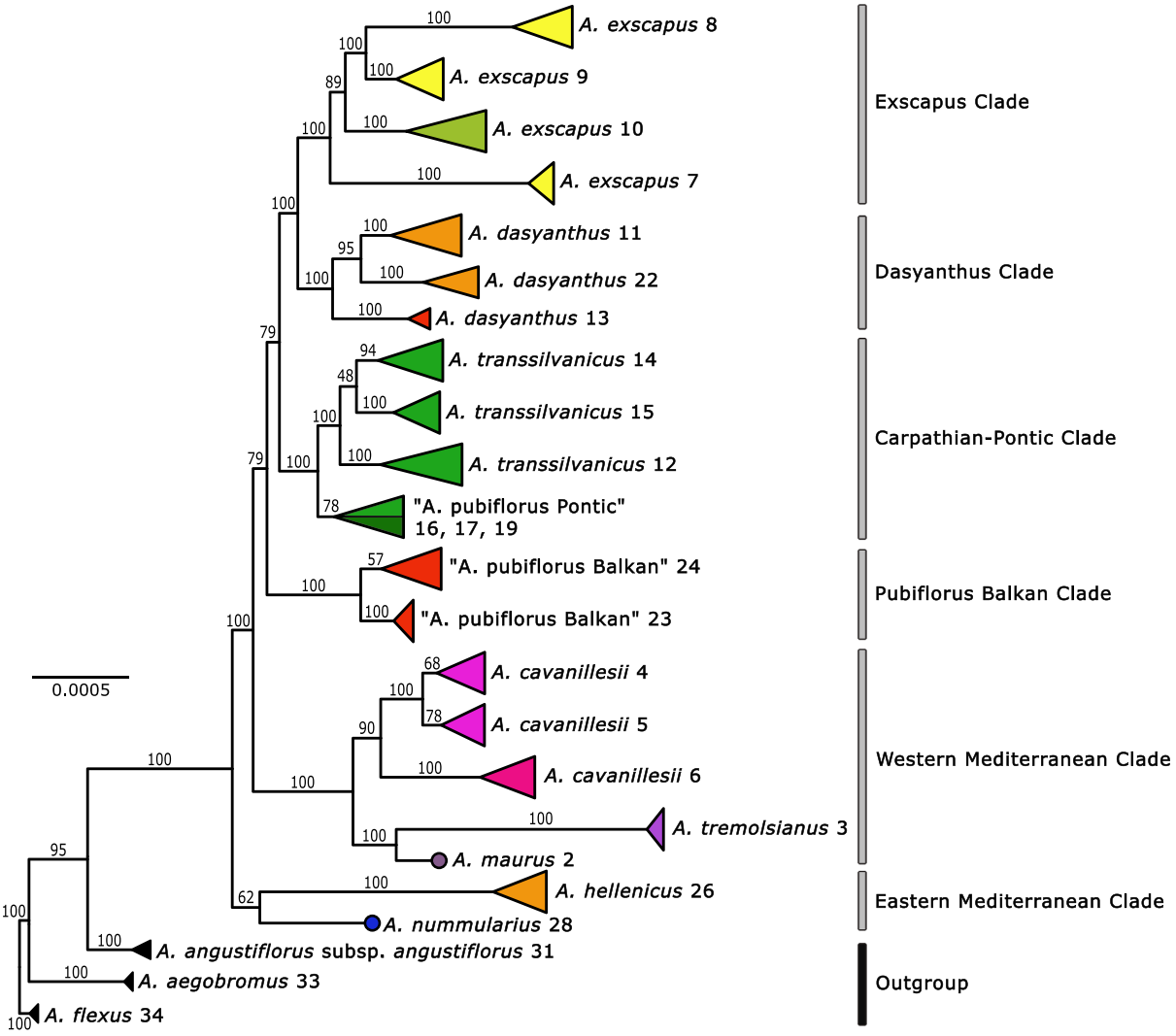

Fig. 3. Maximum likelihood (RAxML) phylogeny of northwestern African and European members of *Astragalus* sect. *Caprini* (AEMAC) and outgroup based on 23,387 SNPs derived from RADseq. Terminal nodes were collapsed for better legibility. Numbers above branches indicate bootstrap support; taxon names are followed by population identifiers (see Supplementary Table S2). Colors of terminals reflect the plastid haplotypes as shown in Fig. 1; populations 2 and 28 are represented by a single individual each.

3.3. Phylogenetic relationships and divergence times based on SNP data

The RADseq dataset included 22 AEMAC populations plus *A. aegobromus*, *A. angustiflorus* and *A. flexus*, which were resolved as closely related outgroups in the plastid (Fig. 1A) and ITS (Fig. 2A) phylogenetic trees. The four replicates clustered with the corresponding individual in the RAxML-tree and the NeighborNet, demonstrating the reproducibility of the method (not shown). The average number of high-quality reads per sample retained after demultiplexing and quality filtering was 2.91 (*SD* = 2.37) million. The denovo_map.pl pipeline identified a mean coverage of 24.31× (± 14.38) over all samples in the catalog. All raw RADseq data are available in the NCBI Sequence Read Archive as BioProject PRJNA1186562 (accession numbers SAMN44766716–SAMN44766620; further details in Supplementary Table S2).

In the RAxML phylogeny rooted with *A. flexus* six main clades were identified within AEMAC with bootstrap values (BS) of 100 %, except for the Eastern Mediterranean Clade (BS 62 %; Fig. 3); backbone nodes received a BS of at least 79 %. AEMAC was resolved as monophyletic and was sister to *A. angustiflorus* subsp. *angustiflorus* (BS 100 %). The Eastern Mediterranean Clade comprising *A. nummularius* and *A. hellenicus* was sister to the other five RADseq clades. The Western Mediterranean Clade consisted of *A. cavanillesii, A. maurus* and *A. tremolsianus*. The Pubiflorus Balkan Clade contained populations of "A. pubiflorus Balkan", and the Carpathian-Pontic Clade comprised "A. pubiflorus Pontic" and *A. transsilvanicus*. Finally, the Exscapus Clade and the Dasyanthus Clade contained populations of *A. exscapus* and *A. dasyanthus*, respectively.

The time-calibrated SNAPP phylogeny including representatives of AEMAC and *A. angustiflorus* subsp. *anatolicus* recovered species as clades with maximum support (PP = 1) except for the split between *A. dasyanthus* and *A. exscapus* (PP = 0.95, Fig. 4). The inferred topology differed slightly from the relationships shown in the RAxML tree (Fig. 3) and the NeighborNet (Fig. 5A). Specifically, the western Mediterranean *A. maurus* was sister to eastern Mediterranean *A. nummularius* and they formed the earliest diverging lineage within AEMAC, followed by *A. hellenicus*. Further, *A. tremolsianus* was nested within *A. cavanillesii* rather than being sister of *A. maurus*. Estimates from three independent runs with two million generations each were consistent and yielded results in a similar range; ESS values exceeded 200 for each parameter. The 95 % HPD intervals of the node ages (numbered in Fig. 4) are given in Supplementary Table S4. The estimated mutation rate was 0.0039 substitutions/site/Ma (95 % HPD: 0.0026–0.0052 substitutions/site/Ma).

The NeighborNet (Fig. 5A) of AEMAC resulted in the recovery of six main groups similar to the lineages resolved by RAxML (Fig. 3), while *A. nummularius* was only loosely linked to *A. hellenicus*.

3.4. Biogeography

In the BioGeoBEARS analyses (Supplementary Fig. 1), models including the *j* parameter fitted best, suggesting that long-distance dispersal events have likely occurred in the evolutionary history of AEMAC. The AIC model selection supported the DIVALIKE + J model, which had a slightly lower AIC value than the DEC + J model in both topologies (AIC-RAxML: DIVALIKE + J = 30.22; DEC + J = 31.86; DIVALIKE = 38.59; DEC = 40.79; AIC-SNAPP: DIVALIKE + J = 34.44; DEC + J = 35.54; DIVALIKE = 45.57; DEC = 51.68). According to the ancestral range estimation, the geographic origin of AEMAC lineages lies in the Eastern Mediterranean mountains (RAxML: 52 %; SNAPP: 60 %). In addition, the results suggest that the inner Alpine dry valleys, the Pannonian Basin, the Pontic Plains and Transylvania were colonized from (sub-)mediterranean mountains (RAxML: 60 %; SNAPP: 73 %). The origin of the Western lowland steppes was less clear; while the analysis based on RAxML supported an origin from the Western Mediterranean

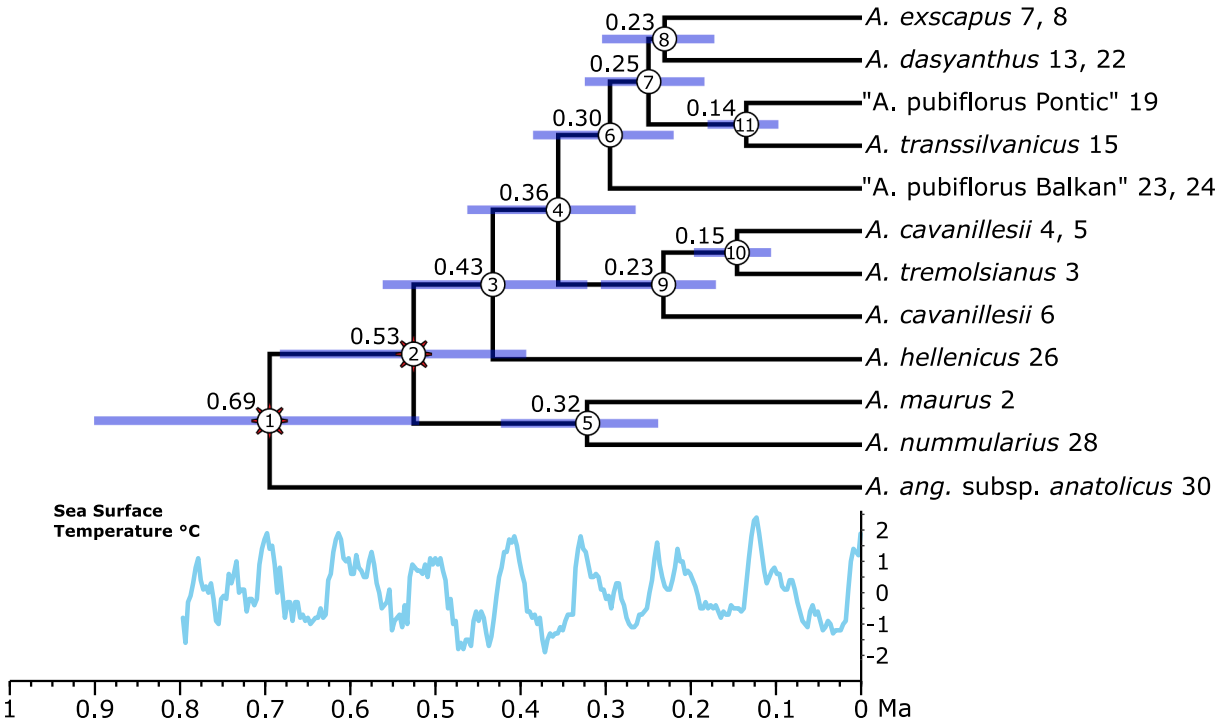

Fig. 4. Time-calibrated phylogeny (maximum clade credibility tree) reconstructed with SNAPP. As a proxy for temperature changes during the last 800,000 years the mean sea surface temperature (°C; Shakun et al., 2015) is indicated above the chronological scale. The phylogeny is based on 9,708 RAD loci illustrating the phylogenetic relationships among northwestern African and European members of *Astragalus* sect. *Caprini* (AEMAC) and their closest relative *A. angustiflorus* subsp. *anatolicus*. Taxon names are followed by population identifiers (see Supplementary Table S2). Numbers above branches are median ages in million years (Ma). All nodes were maximally supported (posterior probabilities, PP = 1) except for node 8 (PP = 0.95). Red stars (nodes 1 and 2) indicate secondary calibration points and blue bars represent 95 % highest posterior densities intervals (details are in Supplementary Table S4). The abbreviation "ang." stands for the species epithet "angustiflorus". (For interpretation of the references to colour in this figure legend, the reader is referred to the web version of this article.)

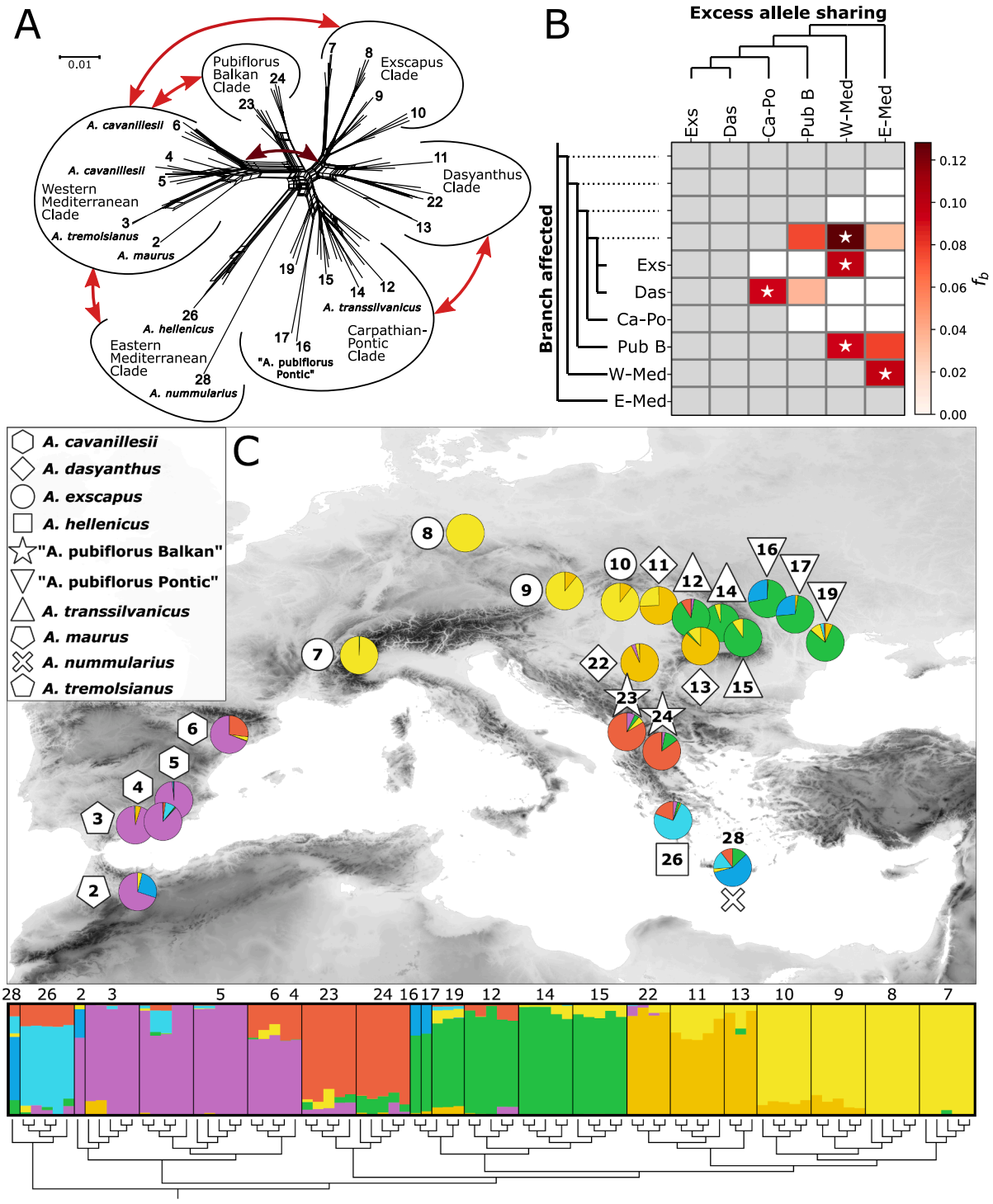

Fig. 5. Genetic structure and gene flow among northwestern African and European members of *Astragalus* sect. *Caprini* (AEMAC). A, NeighborNet based on 251,375 SNPs. Numbers are population identifiers (see Supplementary Table S2), arrows display strongest gene flow between the clades as evidenced by the *f*-branch statistic (values > 0.09 are shown), and colors of arrows correspond to the strength of the signal as indicated in B. The clades resolved in the RAxML phylogeny (Fig. 3) are indicated. B, introgression as estimated by the *f*-branch statistic (summary of *f4* admixture ratios; details are in Supplementary Table S6). The heat map summarizes the *f*-branch statistics estimated in Dsuite. Gray cells indicate inadmissible comparisons due to topological constraints of the underlying phylogeny. White stars highlight the five strongest gene flow events shown in A. Dotted lines in the phylogeny represent ancestral lineages. Ca-Po, Carpathian-Pontic Clade (*A. transsilvanicus*: 12, 14, 15; "A. pubiflorus Pontic": 16, 17, 19); Dasyanthus Clade (11, 13, 22); Exscapus Clade (7–10); E-Med, Eastern Mediterranean Clade (*A. hellenicus*: 26, *A. nummularius*: 28); Pubiflorus B, Pubiflorus Balkan Clade ("A. pubiflorus Balkan": 23, 24); W-Med, Western Mediterranean Clade (*A. cavanillesii* 4–6, *A. maurus*: 2, *A. tremolsianus*: 3). *Astragalus angustiflorus* subsp. *angustiflorus* (31) was used as outgroup. C, Structure analysis results for $K = 7$ clusters, results for other K's are given in Supplementary Fig 3. Pie charts in the map and bar plots show the assignment of populations and individuals, respectively, to each of the seven Structure clusters; populations are separated by black vertical lines in the bar plots. Below the bar plots the RAxML phylogeny (as in Fig. 3) is shown.

mountains (94 %), the analysis based on SNAPP was inconclusive (50 % for an ancestral range in the Western Mediterranean mountains).

3.5. Patterns of gene flow uncovered with ABBA-BABA tests, f-branch statistics and Bayesian clustering

ABBA-BABA tests (Fig. 5B, Suplementary Tables S5 and S6) for the six RADseq groups (based on the RAxML topology; Fig. 3) indicated significant excess of allele sharing for 16 out of the 20 tested trios ($D \neq 0$, $Z > 3$, p-value < 0.05; Supplementary Table S5). *D* statistics for significant trios ranged from 0.26 to 0.08, whereas the highest values were observed between the Western Mediterranean Clade on the one hand and the Exscapus, Dasyanthus, Pubiflorus Balkan and Eastern Mediterranean Clade (Supplementary Table S5) on the other hand. The associated *f*-branch statistic yielded similar results (Fig. 5B, Supplementary Table S6) and additionally uncovered gene flow between the co-occurring Carpathian-Pontic Clade and the Dasyanthus Clade. Two additional ABBA-BABA tests targeting the Western Mediterranean Clade and eastern Mediterranean *A. nummularius* showed significant gene flow within the Iberian Peninsula (both topologies, Supplementary Fig. 2, Supplementary Table S7, Supplementary Table S8) and across the strait of Gibraltar (SNAPP topology, Supplementary Fig. 2, Supplementary Table S7). In only one of the three tested triplets, significant gene flow between western Mediterranean *A. maurus* and eastern Mediterranean *A. nummularius* was found (RAxML topology; Supplementary Fig. 2, Supplementary Table S7).

In the Structure analysis, the optimal number of groups based on delta *K* (Evanno et al., 2005) was two, indicating a separation between the Western Mediterranean cluster and a cluster comprising all other taxa (Supplementary Figs 3, 4). The results at $K = 7$ (Fig. 5C) —the *K*

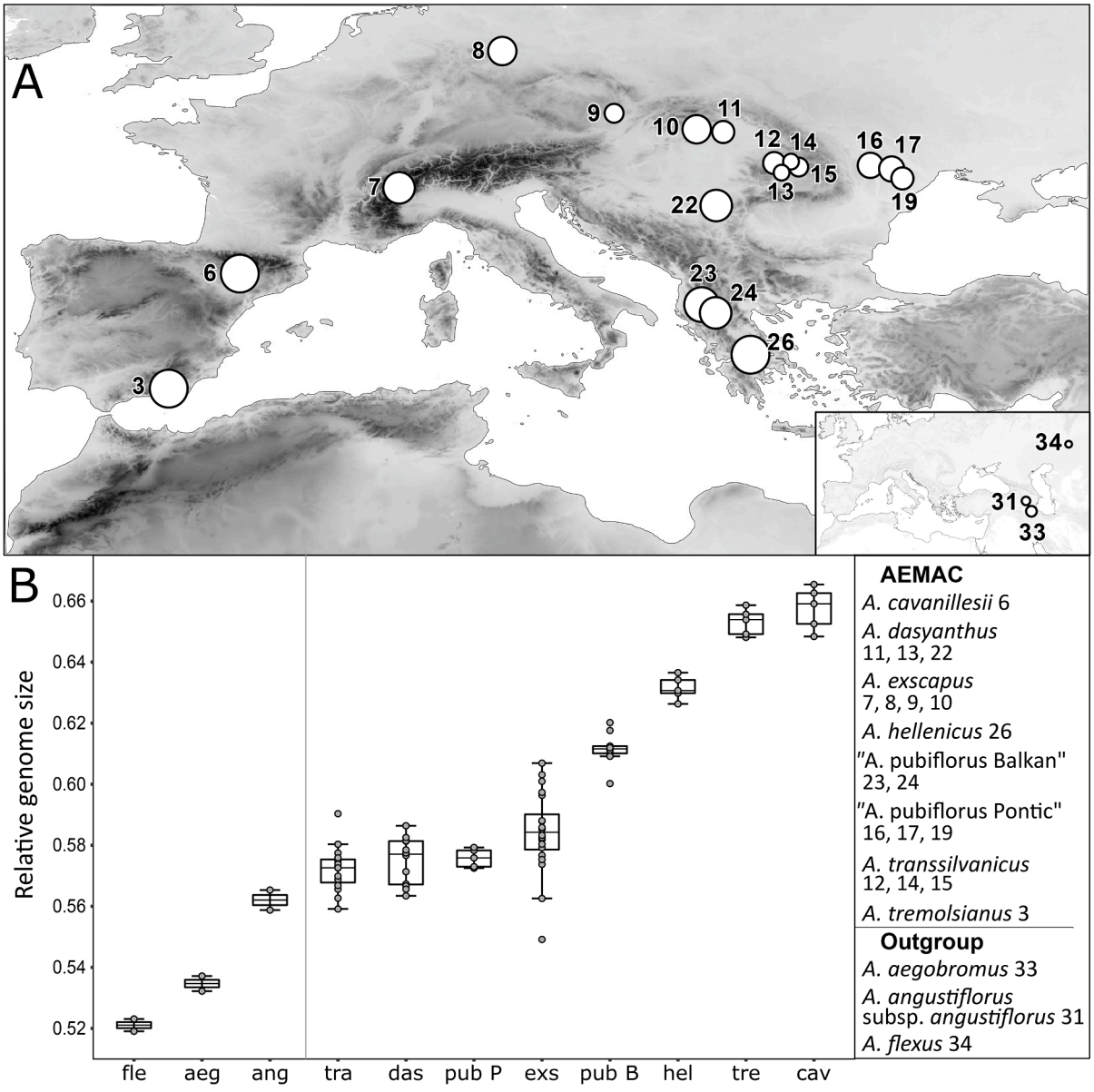

Fig. 6. Relative genome size (RGS) variation of the studied species of *Astragalus* sect. *Caprini*, including northwestern African and European members (AEMAC) and three outgroup taxa. A, geographical distribution of population means of RGS depicted as circles of varying size. The inset shows the distribution and RGS of outgroups. B, RGS variation across the investigated taxa; boxes define 25 and 75 percentiles, horizontal lines indicate medians, whiskers span the 5 and 95 percentiles, grey points indicate individual measurements. Abbreviated taxa names are spelled out in the inset to the right, numbers are population identifiers (Supplementary Table S2).

value after which the likelihood curve flattens (Supplementary Fig. 4)—essentially reflected the groups resolved in the RAxML phylogeny (Fig. 3) and the NeighbourNet (Fig. 5A). All clustering solutions at K = 2–10 are shown in Supplementary Fig. 3. Populations *A. maurus* 2 as well as "A. pubiflorus Pontic" 16 and 17 shared ancestry with geographically distant, early diverging *A. nummularius*. The northernmost population of the Western Mediterranean Clade (*A. cavanillesii* 6) and *A. hellenicus* 26 showed substantial admixture with "A. pubiflorus Balkan". Finally, there was admixture between population *A. dasyanthus* 11 and *A. exscapus*. Less pronounced admixture was found among *A. transsilvanicus*, *A. exscapus*, *A. dasyanthus* and"A. pubiflorus Balkan" as well as between *A. hellenicus* and population 4 of *A. cavanillesii*; due to

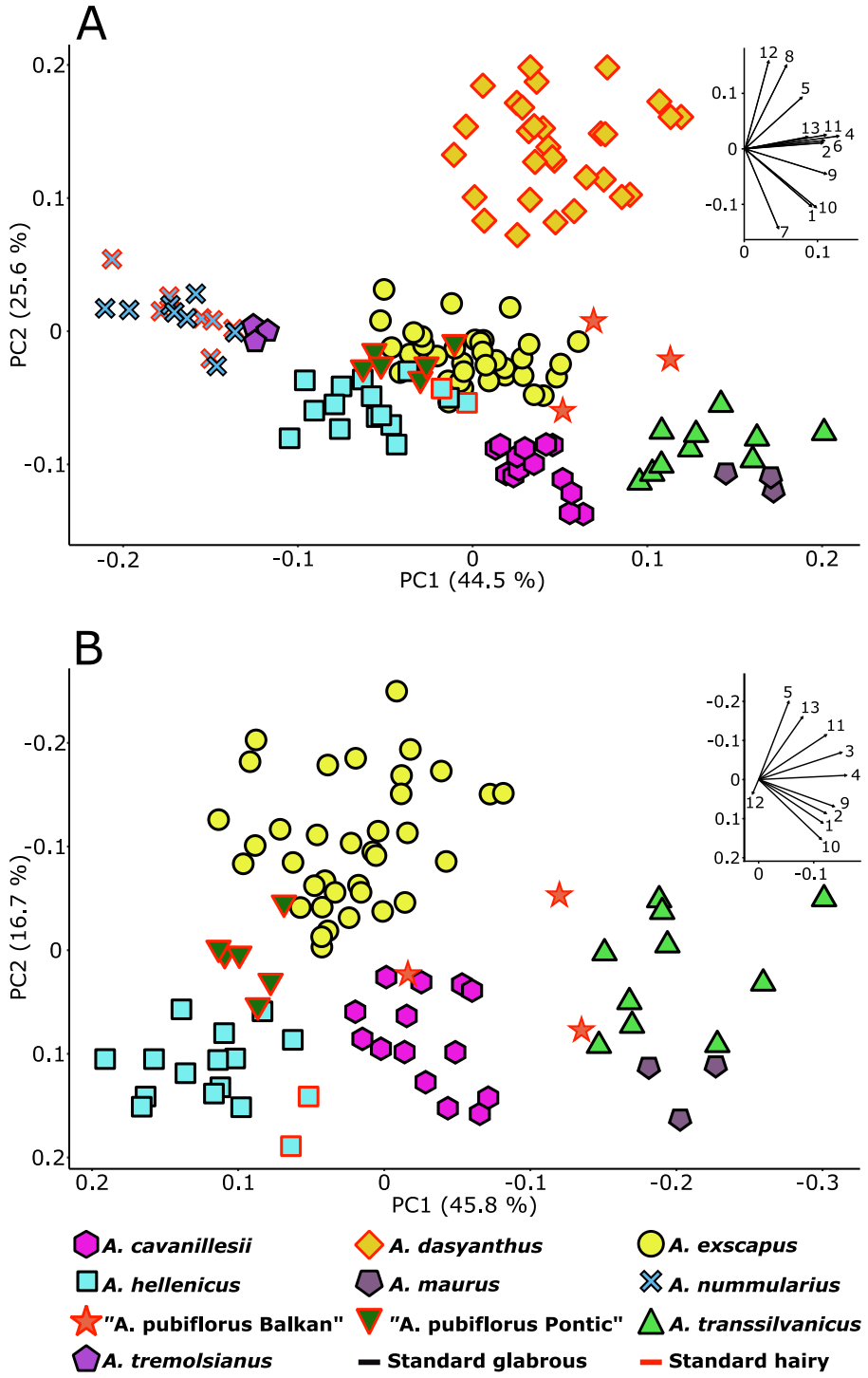

Fig. 7. Morphological variation of northwestern African and European members of *Astragalus* sect. *Caprini* (AEMAC). Red and black outlines indicate whether the abaxial side of the standard is hairy or glabrous. Arrows in the insets represent the contribution of the characters to the overall explained variation; numbers correspond to characters listed in the Materials and Methods. A, PCA based on all AEMAC taxa (137 individuals and twelve characters). B, PCA after exclusion of morphologically most divergent *A. dasyanthus*, *A. nummularius* and *A. tremolsianus* (remaining: 88 individuals) and ten characters providing a better separation of taxa overlapping in A. The plot was mirrored in order to enhance comparability with A. Voucher details are given in Supplementary Table S3. (For interpretation of the references to colour in this figure legend, the reader is referred to the web version of this article.)

this low proportion of admixture, we refrain from discussing these results in detail.

3.6. Relative genome size variation

Within AEMAC, the mean RGS per population ranged between 0.57 (*A. exscapus* 9, *A. dasyanthus* 13, *A. transsilvanicus* 14 and 15, "A. pubiflorus Pontic" 19) and 0.66 (*A. cavanillesii* 6; Fig. 6, Supplementary Table S2), indicating no variation in ploidy level. At the species level, the smallest mean RGS of 0.57 was found in *A. dasyanthus* and *A. transsilvanicus*. The largest mean RGS values were found in "A. pubiflorus Balkan" (0.61), *A. hellenicus* (0.63), *A. tremolsianus* (0.65), and *A. cavanillesii* (0.66). In *A. exscapus* (mean RGS: 0.58), the species with the widest span, individual RGS values ranged between 0.55 in population 9 and 0.61 in population 7. The outgroup taxa *A. angustiflorus* subsp. *anatolicus* 30 and *A. angustiflorus* subsp. *angustiflorus* 31 had a RGS of 0.56–0.57. More distantly related *A. aegobromus* 33, *A. caprinus* subsp. *glaber* 35, *A. multijugus* 47, *A. flexus* 34, and *A.* cf. *sarytavicus* 45 had a RGS of 0.54, 0.59, 0.52, 0.52, and 0.53, respectively (Supplementary Table S2).

3.7. Morphological differentiation

The calculated correlation coefficients did not exceed 0.85 for any character pair. Consequently, no characters were excluded. The PCA of the morphometric dataset, which included all 137 individuals and twelve characters (Fig. 7A) revealed a clear structure. The first two axes explained 44.5 % and 25.6 % of the total variability. *Astragalus dasyanthus, A. nummularius / A. tremolsianus*, *A. cavanillesii* and *A. maurus / A. transsilvanicus* were well separated from each other and from the remaining taxa, which showed strong overlap. The first axis was highly correlated with characters 4, 5 and 6, describing the shape of the middle leaflets and stipule length (11). Floral characters, i. e. hairiness (12) and length (10) of the standard, pedicel length (7) or calyx teeth length (1) were mainly correlated with the second axis. If present, the number of hairs on the abaxial surface of the standard (12) ranged from 5 ("A. pubiflorus Pontic", voucher G00421088_2; *A. nummularius,* voucher G00421096) to 292 (*A. dasyanthus*, voucher B101097557). All examined specimens of *A. dasyanthus*, "A. pubiflorus Balkan" and "A. pubiflorus Pontic" had hairy standards, while in *A. hellenicus* and *A. nummularius* this was the case in 7 out of 15 (46.67 %) and 2 out of 15 (13.33 %) specimens, respectively. The standards of the remaining species (*A. cavanillesii*, *A. exscapus*, *A. maurus*, *A. transsilvanicus* and *A. tremolsianus*) were consistently glabrous (Fig. 7). To further investigate the taxa with overlapping morphometric variability, a second PCA was performed, after exclusion of most divergent *A. dasyanthus*, *A. nummularius* and *A. tremolsianus*. This second approach yielded clear groups with almost no overlap (Fig. 7B), supporting morphological differentiation of the investigated species. Similar to the large dataset, the first axis (45.8 %) was highly correlated with characters describing vegetative parts, i. e. leaf length (3) or length of a middle leaflet (4), whereas generative traits such as hairiness (12) and length of the standard (11) were correlated with the second axis (16.7 %).

4. Discussion

4.1. Initial westward range expansion from (sub-)mediterranean mountains in the Mid-Pleistocene

The northwestern African, southern and central European members of *Astragalus* sect. *Caprini* (AEMAC) form a strongly supported monophyletic group (Figs. 1–4). The RGS data (Fig. 6, Supplementary Table S2) showed no ploidy variation; accordingly, only diploid chromosome counts of $2n = 16$ have been reported so far (*A. dasyanthus*: Pavlova, 1988; *A. exscapus*: Dvořák et al., 1977; Mesícek and Javurková-Jarolímová, 1992, "A. pubiflorus Balkan": $2n = 16 + 2B$, Petrova and Vladimirov, 2020; Pavlova and Tosheva, 2002a; *A. angustiflorus* subsp. *angustiflorus*, Maassoumi, 1989). Within AEMAC, *A. nummularius*, occuring in Crete, Syria and Lebanon was consistently resolved as the earliest-diverging lineage, either as sister to all other AEMAC species (*ycf1* tree, Fig. 1; ITS tree; Fig. 2), or forming a clade together with *A. hellenicus* from southern Greece (RAxML tree, Fig. 3), or with *A. maurus* from northwestern Africa (SNAPP tree, Fig. 4); potential reasons for these incongruences are discussed below. Close relatedness of *A. nummularius* and *A. hellenicus* is reflected also in their morphology; both are small-sized plants with few flowers and with petals whose abaxial surface can be either hairy or glabrous. In contrast, in the other investigated species these character states became fixed (Fig. 7).

The phylogenies retrieved from differentially inherited marker systems as well as the BioGeoBears analyses congruently suggest that the westbound range expansion of AEMAC may have started from western Asia, where most outgroup taxa occur (Figs. 1–4, Supplementary Fig. 1, Supplementary Table S2). Western Asia has been shown to be the center of diversity and a source area for several subgeneric groups within *Astragalus* (Azani et al., 2019; Folk et al., 2024ab; Maassoumi and Ashouri, 2022). A similar West Asian origin of the Mediterranean taxa was recently revealed in the *Euphorbia nicaeensis* All. alliance, which inhabits similar types of grasslands as the members of AEMAC (Stojilkovič et al., 2022). Our findings once again highlight the importance of the Irano-Turanian floristic region as a source area for the colonization of the Mediterranean Basin (Manafzadeh et al., 2017; also see Herrando-Moraira et al., 2023; Ramos-Gutiérrez, 2022) and the Eurasian steppes (Žerdoner Čalasan et al., 2024). The split of AEMAC from its sister *A. angustiflorus* subsp. *anatolicus* was dated to roughly 0.7 Ma (Fig. 1) and coincides with the end of the Mid-Pleistocene Transition (MPT, 1.25–0.7 Ma; Clark et al., 2006; Lisiecki and Raymo, 2007), when cold stages became significantly longer (ca. 100 ky instead of ca. 40 ky), and more intense (Hays et al., 1976; Herbert, 2023). It is noteworthy that in the *A. caprinus* group, the second lineage within *A.* sect. *Caprini* showing westward range expansion to North Africa, divergence times are highly similar to those found in AEMAC (Fig. 1). Specifically, this group diverged from its Irano-Turanian sister *A. urmiensis* 0.8 Ma and subsequently started to diversify 0.4 Ma.

The MPT has likely triggered large-scale expansions of steppes at the expense of forests in Europe and Western Asia, similarly as observed during later glacial stages (Binney et al., 2017). This is reflected in the fossil pollen record (Popescu et al., 2010) and the mammal megafauna associated with the Eurasian steppes that emerged and diversified during and shortly after the MPT (Kahlke, 2014; Kahlke et al., 2011). Similarly, the diversification within AEMAC started between ca. 0.5 Ma and 0.7 Ma (Figs. 1, 2, 4), likely driven by increasingly extreme climatic fluctuations after the MPT (Figs. 1, 4; Supplementary Table S4), supporting a scenario in which climatically-induced contractions and fragmentations of continuous cold-stage steppes during interglacials facilitated allopatric speciation as shown for other steppe species (Brown, 1957; Baca et al., 2023; Kirschner et al., 2023). In this respect, our results are consistent with diversification scenarios described for various Eurasian steppe biota, including vascular plants, insects, and mammals, which also took place during or shortly after the MPT (Baca et al., 2023; Chang et al., 2017; Hodková et al., 2019; Kirschner et al., 2022; Kryštufek et al., 2009; Maylandt et al., 2024; Palkopoulou et al., 2013; Seidl et al., 2022; Sucháčková Bartoňová et al., 2020; Yuan et al., 2023).

4.2. Mountain species diverged earlier than lowland steppe species and have larger genomes

Within AEMAC, present-day range-restricted species occurring in (sub-)mediterranean mountain habitats such as western Mediterranean *A. cavanillesii*, *A. maurus* and *A. tremolsianus* as well as eastern Mediterranean *A. hellenicus*, "A. pubiflorus Balkan" and *A. nummularius* constitute lineages, which, according to the RADseq-based analyses,

diverged earlier than the more northerly distributed, widespread species of lowland steppes such as *A. dasyanthus*, *A. exscapus,* "A. pubiflorus Pontic" and *A. transsilvanicus* (Figs. 1–4). In the same line as the ancestral range estimation conducted with BioGeoBEARS (Supplementary Fig. 1), this strongly supports a transition from mountain habitats to lowland steppes, followed by diversification, as observed within the *A. onobrychis* species complex (Záveská et al., 2019). Mountain ranges are better climatically buffered than lowlands (Scherrer and Körner, 2011) and thus likely acted as refugia, enabling the long-term survival of species by profiting from topographic heterogeneity (Willner et al., 2021), i. e. by tracking of the climatic niche along the altitudinal gradient (Surina et al., 2011), similar to what is observed under current global warming (Chen et al., 2011; Rumpf et al., 2018). In contrast, in lowland steppes, niche tracking forced the biota to shift their ranges over large distances, conferring a strong homogenization of gene pools (Kirschner et al., 2022).

Reflecting their phylogenetic divergence, (sub-)mediterranean mountain species such as *A. cavanillesii*, *A. hellenicus*, "A. pubiflorus Balkan" and *A. tremolsianus* show a tendency towards larger genomes and strong RGS differentiation across species. In contrast, the four closely related lowland steppe lineages *A. dasyanthus*, *A. exscapus*, "A. pubiflorus Pontic" and *A. transsilvanicus* have similarly smaller genomes (Fig. 6). The RGS was larger in members of AEMAC than in the distantly related outgroup species from western and central Asia (Fig. 6, Supplementary Table S2), while both subspecies of *A. angustiflorus*, most closely related to AEMAC (Figs. 1–4) and distributed from the southern Caucasian area to western Anatolia, had a RGS at the lower end of the variation within AEMAC (Fig. 6, Supplementary Table S2). The exact causes for the observed RGS variation are elusive, but differences in the amount of retrotransposons and other repetitive elements have been considered the main cause of GS variation in angiosperms (Pellicer et al., 2018). Additionally, a previous study indicated the presence of two B chromosomes in "A. pubiflorus Balkan" (Pavlova and Tosheva, 2002a), which may have also contributed to the observed RGS variation among taxa.

4.3. The origin of western Mediterranean species is complex and difficult to elucidate

The divergence of western Mediterranean lineages occurred early in the evolution of AEMAC (0.5–0.3 Ma; Figs. 1–3), but their origin is intricate and challenging to reconstruct. Specifically, although the western Mediterranean species form a well-resolved group in the NNet (Fig. 5A), a maximally supported monophyletic clade in the RAxML phylogeny (Fig. 3), and constitute a genetic cluster identified by the Structure analysis at $K = 2$–10 (Fig. 5C, Supplementary Fig. 3), monophyly of the Western Mediterranean Clade was not congruently resolved. For example, the ribotype of *A. maurus* diverges early (0.5 Ma) and does not group with the younger (0.3 Ma) members of the Western Mediterranean Clade, which all had the "common ribotype" in the ITS tree (Fig. 2). Furthermore, *A. maurus* and *A. tremolsianus* belong to an earlier diverging clade (0.5 Ma) and do not cluster with monophyletic *A. cavanillesii* in the plastid tree (0.4 Ma; Fig. 1). Additional incongruence was revealed by the SNAPP analysis (Fig. 4), which resolved *A. maurus* as sister to earliest-diverging *A. nummularius*, an ancestral connection also indicated by the Structure analysis (Fig. 5C, Supplementary Fig. 3), while *A. tremolsianus* was nested within later diverging (0.4 Ma) *A. cavanillesii*. Incongruence within the Western Mediterranean Clade can be partly caused by gene flow among its members, as revealed by the ABBA-BABA analyses (see section 4.5, Supplementary Fig. 2, Supplementary Table S7 and S8; Mallet et al., 2016). However, as incongruences of RADseq-based analyses could arise from both biological as well as methodological factors (Fleming et al., 2023; Hühn et al., 2022; Wagner et al., 2020), formulating an unequivocal hypothesis for the origin of the Western Mediterranean Clade is challenging. Since incongruence involves western and eastern Mediterranean species, we speculate that these conflicting patterns and the signals of admixture discussed below (see section 4.5, Fig. 5) might indicate that the Iberian Peninsula was colonized at different time horizons by at least two independent immigrations of AEMAC lineages from the eastern Mediterranean. This reflects scenarios outlined for other plant groups, where close evolutionary links were found between early diverging lineages occurring in the western and eastern extremes of the Mediterranean Basin (*Erophaca baetica*, Casimiro-Soriguer et al., 2010; *Astragalus* sect. *Tragacantha*, Hardion et al., 2016; *Myrtus communis*, Migliore et al., 2012; reviewed by Nieto Feliner, 2014).

Whether range expansion to the western Mediterranean was facilitated by stochastic long-distance dispersals (Nathan, 2006), or rather involved continuous range expansion during the cold stages of the Pleistocene cannot be safely inferred based on our results. According to the BioGeoBEARS analyses (Supplementary Fig. 1), we cannot rule out that the evolution of AEMAC involved long-distance dispersals, and the occurrence of *A. nummularius* in Crete and the close relationship between *A. maurus* and *A. tremolsianus,* which are separated by the Strait of Gibraltar, clearly demonstrate a certain ability of AEMAC for transoceanic dispersal. Previous studies have shown that long-distance dispersals have occurred in *Astragalus* despite of relatively heavy seeds (Bobo-Pinilla et al., 2021, 2018; Folk et al., 2024b), even bridging the Atlantic (Azani et al., 2019). Whereas the exact mechanism of dispersal (abiotic or biotic) remains unclear, it is noteworthy that *Astragalus* DNA was identified in the content of the digestive system of different extinct megaherbivores, including wholly mammoths (van Geel et al., 2008; Axmanová et al., 2020). Additionally, recent findings indicate that *Astragalus* seeds can survive the gut passage of large mammals (Jaganathan et al., 2019; Trabelsi et al., 2023) and were indeed found in the digestive system and dung of different animals (Ghasemi et al., 2024; Houghton et al., 2020; Lovas-Kiss et al., 2015); suggesting their potential role as vectors.

4.4. Mid-Pleistocene colonization of steppe habitats in central and eastern Europe

Central and eastern European lowland steppes as well as the inner-Alpine valleys were likely colonized from the eastern Mediterranean in the Mid-Pleistocene; the split between mountain-dwelling "A. pubiflorus Balkan" and the lowland steppe AEMAC was dated to 0.22 (*ycf1*; Fig. 1) or 0.30 Ma (SNAPP; Fig. 4). *Astragalus dasyanthus* and *A. exscapus* diverged roughly at the same time (0.23 Ma, Fig. 4), while "A. pubiflorus Pontic" and *A. transsilvanicus* separated later (0.14 Ma, Fig. 4). These results support a fairly recent colonization of the Pontic Plains by *A. dasyanthus* and "A. pubiflorus Pontic" and reject the classical biogeographical assumption of an east-to-west colonization of the Pannonian-Pontic steppes (De Soo, 1929), a scenario also hypothesized for the steppe beetle *Lethrus apterus* (Sramkó et al., 2022). This highlights the importance of extrazonal refugia such as the Pannonian Basin and the Balkan Mountains for steppe organisms with a broad, zonal-extrazonal distribution, further emphasizing the high conservation value of extrazonal steppes (Kirschner et al., 2020). Interestingly, recently evolved *A. exscapus* and *A. dasyanthus* did not only hybridize where they co-occur (Fig. 5C, Supplementary Fig. 3); they also show signals of strong gene flow with the Western Mediterranean Clade, suggesting a past connection (discussed below; Fig. 5AB). Populations of *A. dasyanthus* from the Pannonian Basin have the same plastid haplotype as *A. hellenicus* (Figs 1, 3) and the Carpathian-Pontic populations of *A. dasyanthus* shared the haplotype with "A. pubiflorus Balkan" (Fig. 1). These connections were also found by the ABBA-BABA test (Fig. 5B, Supplementary Table S5 and S6). Sharing of haplotypes and the indicated gene flow between these species, which are distantly related in the RADseq phylogenies (Figs 3, 4), hints at incomplete lineage sorting or hybridization ("chloroplast capture"; Petit et al., 2004; Rieseberg and Soltis, 1991), as well supporting a scenario of recurring secondary contacts among divergent AEMAC lineages.

4.5. Secondary contacts co-shaped the genetic structure of AEMAC

Climate-mediated rapid and large-scale range expansions and contractions have had an important impact on the diversification of Eurasian steppe biota (Kirschner et al., 2020; 2023). Our results suggest that these dynamics have also played an important role in the diversification of AEMAC. This is reflected by incomplete lineage sorting and recurrent gene flow between diverging lineages, processes which are well known from other plant groups (Cai et al., 2021; Rose et al., 2021; Stojilkovič et al., 2022). Secondary contacts during cold-stage range expansions of currently spatially isolated lineages likely co-shaped the genetic structure of AEMAC, which is supported by both Structure and ABBA-BABA analyses (Fig. 5, Supplementary Tables S5 and S6). It has been suggested that Mid- to Late-Pleistocene dynamics stimulated admixture (Anderson and Stebbins, 1954; Folk et al., 2018, 2023; Hewitt, 2011), a pattern also found in various Eurasian steppe organisms (Bartha et al., 2013; Sinaga et al., 2024; Tukhbatullin et al., 2023; Van Der Valk et al., 2021; Záveská et al., 2019). While admixture in the Structure analysis could be related to sampling biases or incomplete lineage sorting (Fig. 5C; Meirmans, 2018; Puechmaille, 2016), ABBA-BABA analyses clearly supported an important role of gene flow in AEMAC (Fig. 5B; Patterson et al., 2012)

The results of large-scale range expansions and contractions in AEMAC can be observed as secondary contacts between nowadays isolated lineages. Striking examples are the strong signal between (1) eastern Mediterranean "A. pubiflorus Balkan" and western Mediterranean *A. cavanillesii* or (2) between the eastern lowland species *A. dasyanthus, A. exscapus* and/or their common ancestor and the western Mediterranean species (Fig. 5, Supplementary Table S5). In this respect, long-distance dispersals might have also played a role (see section 4.3).

At a smaller geographic scale, we found evidence of gene flow between recently evolved species with overlapping distribution ranges, a widely observed pattern found in many other systems (Malinsky et al., 2018; Mallet, 2005; Soltis and Soltis, 2009). For example, the signals of gene flow between *A. dasyanthus* and *A. exscapus* or between *A. dasyanthus* and members of the Carpathian-Pontic Clade. Within the Western Mediterranean Clade, gene flow was detected between *A. cavanillesii* and *A. tremolsianus* occurring in close vicinity in the southern Iberian Peninsula and between *A. maurus* and *A. tremolsianus* (Supplementary Fig. 2, Supplementary Tables S7 and S8). The latter indicates a connection across the Strait of Gibraltar, which has already been shown to be permeable to gene flow in some plant groups (Bobo-Pinilla et al., 2018; Bougoutaia et al., 2021; Nieto Feliner, 2014; Gil-López et al., 2022; Guzmán and Vargas, 2009; Martín-Rodríguez et al., 2020).

4.6. Towards a revised taxonomic framework for European members of *A. sect. Caprini*

Our study shows that an integrative approach, which combines complementary methods, can successfully resolve relationships within a recently evolved and widespread group, for which controversial taxonomic treatments exist (Podlech 2011, 1988; Podlech and Zarre, 2013; Strid and Tan, 1997; Supplementary Table S1). In contrast to previous phylogenetic studies that only used Sanger sequencing to investigate relationships and to make taxonomic claims on members of sect. *Caprini* or closely related groups (i. e. sect. *Alopecuroidei*) within the Phaca clade (Javanmardi et al., 2012; Riahi et al., 2011; Sheikhakbari-Mehr and Maassoumi, 2017), we were able to formulate robust hypotheses about interspecific relationships of a recently emerged group by using RADseq and the plastid marker *ycf1*. This highlights the importance of molecular approaches based on a high number of single nucleotide polymorphisms (SNPs) and/or highly variable markers to investigate phylogenetic relationships on inter- and intraspecific levels in *Astragalus*, which experienced parallel diversification bursts in several clades at the onset of the Pleistocene and around and after the MPT (Azani et al., 2019; Folk et al., 2024b; Su et al., 2021; Záveská et al., 2019; Figs. 1, 2, 4). Discrimination among AEMAC species was not possible with ITS, due to the recent divergence of lineages and the pace of the mutation rate, which was approximately three times slower in ITS compared to *ycf1* (see Results; section 3.1, 3.2). Highly similar results were found in the steppe plant *A. austriacus* (Maylandt et al., 2024).

Based on the presented morphometric, genetic and genomic data, we suggest treating the ten AEMAC lineages introduced in this study as independent species. This stands in stark contrast to the previous taxonomic treatment by Podlech and Zarre (2013), where *A. exscapus* was broadly circumscribed to include *A. hellenicus*, *A. transsilvanicus*, the northernmost population of *A. cavanillesii* (population 6, Figs. 1, 5; Ferrández Palacio, 2003) and the westernmost populations of "A. pubiflorus Pontic" from the Pontic steppes (Ukraine, Romania). We show that *A. hellenicus* does not overlap morphologically with *A. exscapus* (Fig. 7B); according to the RADseq data it is, alongside morphologically similar *A. nummularius,* one of the earliest-diverging lineages within AEMAC species (Figs. 3, 4) and also differs in RGS (Fig. 6). Similarly, *A. transsilvanicus*, endemic to the Transylvanian Basin, is morphologically and phylogenetically divergent from *A. exscapus* (Figs. 3, 4, 7) and is phylogenetically most closely related to geographically close "A. pubiflorus Pontic" (Figs. 1–4). It is noteworthy that ca. 85 % of the populations of *A. transsilvanicus* were driven to extinction over the last 200 years and only 24 recent populations are known today, illustrating the taxon's massive and very immediate threat (Bădărău et al., 2000, 2001).

4.7. Unexpected sister relationship between morphologically dissimilar *A. dasyanthus and A. exscapus*

A strong argument to treat the investigated AEMAC entities as separate species is the fact that *A. dasyanthus*, the only caulescent and thus morphologically most divergent species within AEMAC, for which species status was always beyond any doubt, is among the later-diverging species (Fig. 4); it was resolved as sister to *A. exscapus* in all genetic analyses (Figs. 1, 3, 4, 5A, 7A). Its position in the phylogenetic trees indicate that *A. dasyanthus* is the only AEMAC that reversed to the ancestral, caulescent growth form exhibited by taxa outside *A.* sect. *Caprini.* This probably implies that this conspicuous difference has a simple genetic basis. Indeed, the acaulescent (stemless) habit is typical for members of *A.* sect. *Caprini* and can be considered a synapomorphy of this section, with reversal in *A. dasyanthus*. We speculate that this unique morphological feature may cause a later and prolonged flowering of *A. dasyanthus* (Maylandt, personal field observations), allowing its sympatric occurrence with – likely cross-compatible – members of this group, such as *A. exscapus*, "A. pubiflorus Balkan", "A. pubiflorus Pontic" and *A. transsilvanicus*. The early divergent lineages within the "Phaca Clade", i. e. members of *A.* sect. *Alopecuroidei* or *A.* sect. *Cenantrum* (as circumscribed by Su et al., 2021) have well-developed stems. Obviously, low growth and positioning of the apical shoot meristems close to the ground may be beneficial in biomes with strong grazing pressure such as steppes (Díaz et al., 2007). In addition to the strong differentiation in plant habit, the densely hairy petals of *A. dasyanthus* contribute further to the strong morphological differentiation from its sister *A. exscapus*, which has glabrous petals.

4.8. Resolving the taxonomic confusion associated with *A. pubiflorus*

In the past, the distinction between *A. pubiflorus* and *A. exscapus* was contradictory across treatments in terms of both morphology and distribution range (Supplementary Table S1). This is mainly because "A. pubiflorus Pontic" occasionally possesses sparsely hairy to glabrous petals, which led to the wrong interpretation that such individuals belong to *A. exscapus* (Becker, 2010; Ciocârlan, 2000; Fedorov et al., 2002; Goncharov et al., 1946; Podlech, 1988; Podlech and Zarre, 2013;

see Supplementary Table 1). Similarly, populations of *A. pubiflorus* from the southern Balkan Peninsula have been mistaken for *A. exscapus* (Barina, 2017) or have been either treated as *A. exscapus* subsp. *pubiflorus* (Pils, 2016; Podlech, 1988; Podlech and Zarre, 2013; Strid and Tan, 1997; Strid, 2024) or *A. pubiflorus* (Fedorov et al., 2002; Goncharov et al., 1946; Qosja et al., 1992; see Supplementary Table 1). In contrast to all previous taxonomic treatments of *A. pubiflorus*, our results show that the taxon in the traditional circumscription is polyphyletic and should therefore be split into two allopatric species corresponding to "A. pubiflorus Pontic" and "A. pubiflorus Balkan". A formal description of "A. pubiflorus Balkan" based on a more comprehensive sampling is underway (Maylandt et al., in prep.). As the type specimen of *A. pubiflorus* pertains to "A. pubiflorus Pontic", no nomenclatural changes are needed for that entity.

4.9. Revised distribution ranges of *A. cavanillesii* and *A. exscapus* directly bear on the species' actual threat

Western Mediterranean *A. cavanillesii*, *A. tremolsianus* and *A. maurus* should be retained in the current circumscription (Talavera and Castroviejo, 1999) with the exception of population 6 that is clearly *A. cavanillesii* (Figs. 1, 3–4, 7) but was previously treated as *A. exscapus* (Podlech, 2011; Talavera and Castroviejo, 1999). This change implies an increase in the distribution area and number of known populations of *A. cavanillesii*, originally considered a critically endangered species restricted to two single populations in the southern Iberian Peninsula (Sánchez-Gómez et al., 2004). Consequently, its conservation status should be re-evaluated. *Astragalus tremolsianus* is covered by the Council Directive 92/43/EEC on the conservation of European natural habitats and of wild fauna and flora, protected at national level, and has a conservation and management plan from the Andalusian government. The third Western Mediterranean AEMAC species *A. maurus* is not protected, but a conservation assessment is necessary as it is a rare and narrow endemic (Fougrach et al., 2007; Romo, 2002).

Obviously, the proposed taxonomic changes confer a strong reduction of the range of *A. exscapus*, which was previously thought to be widespread. As outlined above, the single Iberian population previously included in *A. exscapus* rather pertains to *A. cavanillesii,* and the mountain-dwelling populations from the western Balkans (="A. pubiflorus Balkan") and southern Greece (=*A. hellenicus*) in fact belong to other species. The same applies to *A. transsilvanicus* and widespread "A. pubiflorus Pontic", which were sometimes included in *A. exscapus*. Altogether, our re-evaluation of the species' range suggests that *A. exscapus* is more range-restricted than assumed previously, which directly bears on the future conservation and protection status of this threatened and declining species (Barina et al., 2007; Becker and Voß, 2003; Schnittler and Günther, 1999; Schratt-Ehrendorfer et al., 2022; Stevanović et al., 1999; Wilhalm and Hilpold, 2006). A detailed study on the spatiotemporal diversification and past population dynamics of *A. exscapus* based on a comprehensive range-wide sampling is underway (Maylandt et al., in prep.). Below, we provide a revised taxonomic treatment of the investigated members of AEMAC, modified from Podlech and Zarre (2013), including an identification key. We only list the most important synonyms; for the complete list see Podlech (2011) or Podlech and Zarre (2013).

4.10. Key to the investigated northwestern African and European members of *Astragalus* sect. *Caprini**

1	Plants with a distinct, (2.9)7.3–14.0(17.3) cm long stem, petals always densely hairy (Pannonian Basin, Transylvania, Pontic Plains) ***A. dasyanthus***
1*	Plants acaulous or with a short, maximally 3.8(4.5) cm long stem, petals glabrous or sparsely hairy **2**
2	Petals at least partially appressed-hairy, hairs sometimes sparse to rarely absent **3**
2*	Petals glabrous **6**
3	Small plants with (1)2–4(5) flowers per inflorescence and (2)3–12(14) flowers per individual, leaf length (25)47–126(140) mm, leaflet length (3.3)3.9–11.0 (12.8) mm and stipule length (4.5)5.9–10.0(11.3) mm **4**
3*	Larger plants with (3)4–6(8) flowers per inflorescence and (9)11–37(60) flowers per individual, leaf length (75)119–337(380) mm, leaflet length (10.8)13.1–28.9(32.0) mm, stipule length (8.1)13.8–18.8(19.8) mm **5.**
4	Standard (21.6)22.0–26.0(28.9) mm long (southern Greece) ***A. hellenicus***
4*	Standard (12.6)13.4–18.0(21.4) mm long (Crete, Levant) ***A. nummularius***
5	Number of lateral leaflets (16)18–22(24), ratio of leaflet length/leaflet width (2)2.1–2.4(2.5), stipule length (8.1)9.8–13.9(14.0) mm (Pontic Plains) **"A. pubiflorus Pontic"**
5*	Number of lateral leaflets (22)24–30(32), ratio of leaflet length/leaflet width (1.49)1.55–2.06(2.37), stipule length (13.4)15.6–18.9(19.8) mm (Albania, northern Greece) **"A. pubiflorus Balkan"**
6	Small plants with (1)2–4(5) flowers per inflorescence and (2)3–12(14) flowers per individual, leaf length (25)47–126(140) mm, leaflet length (3.3)3.9–11.0 (12.8) mm, stipule length (4.5)5.9–10.0(11.3) mm **7**
6*	Medium to large plants with (3)4–7(8) flowers per inflorescence and (6)13–45 (107) flowers per individual, leaf length (89)147–286(350) mm, leaflet length (8.6)11.0–23.9(31.3) mm, stipule length (8.8)12.4–19.7(28.5) mm **9**
7	Standard (21.6)22.0–26.0(28.9) mm long (southern Greece) ***A. hellenicus***
7*	Standard (12.6)13.5–19.0(21.4) mm long **8**
8	Calyx length (7.5)9.1–11.1(11.7) mm, stipule length (4.4)4.6–7.8(7.9) mm (Crete, Levant) ***A. nummularius***
8*	Calyx length (11.6)11.8–12.6 mm, stipule length (9)9.1–10.4(10.6) mm (southern Spain, Sierra de Gador) ***A. tremolsianus***
9	Large plants, leaf length (207)222–316(350) mm, leaflet length (20.1) 20.7–27.6(31.3) mm, standard length (25.3)27.2–30.2(31.0) mm, pedicel length (4.1)4.9–7.1 mm, petiolule length (1)1.3–1.7(1.9) mm, stipule length (13.0)16.1–22.8(28.5) mm, calyx length (17.2)17.7–21.3(21.9) mm, calyx teeth length (8.8)8.9–11.1(11.5) mm, densely to sparsely hairy **10**
9*	Medium to larger plants, leaf length (89)140–243(311) mm, leaflet length (8.6)10.9–17.0(20.9) mm, standard length (18)20.5–26.2(28.9) mm, pedicel length (2.9)3.6–8.0(10.3) mm, petiolule length (0.3)0.5–1.4(1.6) mm, stipule length (8.8)12.1–18.8(22.9) mm, calyx length (11.9)12.6–16.6(20.3) mm, calyx teeth length (5.1)5.6–8.0(9.9) mm, hairy **11**
10	Plants densely covered with hairs (Morocco) ***A. maurus***
10*	Plants sparsely covered with hairs (Transylvania) ***A. transsilvanicus***
11	Petiolule length (1)1.1–1.4(1.6) mm, pedicel length (5.7)6.1–9.1(10.3) mm, number of lateral leaflets (12)16–24(26) (southeastern Spain: Sierra de la Sagra, northeastern Spain: Huesca) ***A. cavanillesii***
11*	Petiolule length (0.3)0.5–0.9(1) mm, pedicel length (2.9)3.5–5.8(7.6) mm, number of lateral leaflets (22)26–30(32) (Alps, Apennines, Germany, Pannonian Basin) ***A. exscapus***

* for "A. pubiflorus Balkan", we used the values from a more comprehensive dataset collected in 2024.

4.11. Revised txonomic treatment of the investigated northwestern African and European members of *Astragalus* sect. *Caprini*

A. cavanillesii Podlech, Mitt. Bot. Staatss. München 25: 161. 1988. Holotype: [Spain] Prov. Granada, La Puebla de Don Fadrique, 1200 m, vi. 1900, *E. Reverchon* 1185 (WU!; iso: B!, BP!, E!, JE!, M SB!, P!, PRC!, Z!). *A. exscapus sensu* Ferrández Palacio (2003). **Distribution:** Southeastern (Sierra de la Sagra) and northeastern Spain (Huesca).

A. dasyanthus Pall., Reise Russ. Reich. 3: 749. 1776 ≡ *Tragacantha dasyantha* (Pall.) Kuntze, Revis. Gen. 2: 944. 1891. Type: [Russia (European part] ad Ilowlam et Medwedizam, *P.S. Pallas* (BM!). **Distribution:** Bulgaria, Georgia, Hungary, Moldova, Romania, Russia (European part), Serbia, Ukraine.

A. exscapus L., Mantissa Alt.: 275. 1771 ≡ *Tragacantha exscapa* (L.) Kuntze, Rev. Gen. 2: 944. 1891. Holotype: [Germany] Thuringia, *Schreber* (LINN!; iso: M!). **Distribution:** Austria, Czech Republic, Germany, Hungary, Italy, Serbia, Slovakia, Switzerland.

A. hellenicus Boiss., Fl. Or. 2: 292. 1872 ≡ *Tragacantha hellenica* (Boiss.) Kuntze, Revis. Gen. 2: 945. 1891 ≡ *A. angustiflorus* K. Koch subsp. *hellenicus* (Boiss.) Ponert, Feddes Repert. 83: 622. 1973. Lectotype: designated by Podlech (1988): [Greece] Parnes Atticae, v. 1842, *E. Boissier* (G-BOIS!; iso: C!, P!). **Distribution:** Endemic to southern

Greece.

A. ictericus Dingler, Flora 64: 381. 1881. Lectotype: (Podlech, Mitt. Bot. Staatss. München 25: 200. 1988): [Greece] pr. Kosluköi Thraciae, 3.5.1876, *H. Dingler* (M!: foto MSB!); the original material at B is destroyed. **Distribution:** Endemic to northern Greece.

A. maurus (Humb. & Maire) Pau in sched. ad Font Quer, It. Marocc. 1929, n 71. 1930 ≡ *A. exscapus* L. subsp. *maurus* Humb. & Maire, Mém. Soc. Sci. Nat. Maroc 15: 26. 1926. Lectotype, designated by Podlech (1988): [Morocco] Daya Ciker audessus de Taza, 1400—1500 m, 25.6.1925, *H. Humbert* (RAB!; iso: MPU!, P!). **Distribution:** Endemic to Morocco.

A. nummularius Lam., Encycl. Méth. Bot. 1: 317. 1783 ≡ *Tragacantha nummularia* (Lam.) Kuntze, Revis. Gen. 2: 946. 1891. Lectotype, designated by Podlech, (1988): [Greece] A. creticus nummulariifolio, incano magno fructu, Creta, *J.P. de Tournefort* (P-TRF 3618!; isolectotypes: B-W 14039!, LE!, MPU!, P: hb. Vaillant!, P-LA!). **Distribution:** Crete (Greece), Levant (Lebanon, Syria).

A. pubiflorus DC., Astragalogia: 216. 1802 ≡ *Tragacantha pubiflora* (DC.) Kuntze, Revis. Gen. 2:947. 1891. Holotype: Habitat in Sibiria e herb. Desfontaines, [*Astragalus pubiflorus* Decand. Astrag. n 111 (scripsit Desfontaines)] (P!). **Distribution:** Endemic to the Pontic region: eastern Romania, Moldova, Russia (European part), Ukraine, (Bulgaria?).

A. transsilvanicus Schur, Verh. Naturf. Vereins Brünn 15: 2. 1876 [et l.c.: 184. 1877. Lectotype, designated by Podlech (1988): [Romania] In collibus apricis bei Egerbergy, 1.5.1873, *J. Barth* ex hb. Schur (P!). **Distribution:** Endemic to Transylvania (Romania).

A. tremolsianus Pau, Mem. Mus. Ci. Nat. Barcelona, Ser. Bot. 1(3): 17. 1925. Holotype: [Spain, prov. Almeria] Sierra de Gador, *Tremols.* **Distribution:** Endemic to the summit region of the Sierra de Gador, southern Spain.

CRediT authorship contribution statement

Clemens Maylandt: Writing – review & editing, Writing – original draft, Visualization, Validation, Software, Methodology, Investigation, Funding acquisition, Formal analysis, Data curation, Conceptualization. **Philipp Kirschner:** Writing – review & editing, Methodology. **Daniela Pirkebner:** Methodology. **Božo Frajman:** Writing – review & editing, Supervision, Investigation, Conceptualization. **Julio Peñas de Giles:** Writing – review & editing. **Peter Schönswetter:** Writing – review & editing, Supervision, Resources, Project administration, Funding acquisition, Conceptualization. **Pau Carnicero:** Writing – review & editing, Supervision, Methodology, Conceptualization.

Declaration of competing interest

The authors declare that they have no known competing financial interests or personal relationships that could have appeared to influence the work reported in this paper.

Acknowledgements

We thank all colleagues listed as collectors in Supplementary Table 2 that provided samples. Special thanks to László Bartha, who made samples of *A. nummularius*, *A. pubiflorus* and *A. exscapus* available. Arne Strid shared locality data of *A. hellenicus* from Flora Hellenica Database, Mihai Puşcaş the locality data of *A. transsilvanicus* and *A. dasyanthus* for Transylvania. We also thank András Schmotzer, Johannes Würtl, Milan Danilović and Nevena Kuzmanović who helped with the collection of samples in southeastern Europe. We are grateful to the curators of the herbaria BC, B, IB, M, MSB, MA, and W for the loan of herbarium specimens. We owe gratitude to Fabian Schafferer and Lara Leiter, who conducted a significant part of the morphometric measurements as part of their Bachelor's theses; further measurements were done by Elias Nitz. Thanks to Markus Möst for sharing his knowledge concerning the ABBA-BABA test and thanks to Jean Nicolas Haas for sharing his expertise on paleoecology. We thank the gardeners of the Botanical Garden of the University of Innsbruck for successfully cultivating our living collection of *Astragalus* species. The computational results presented here have been achieved in part using the LEO HPC infrastructure of the University of Innsbruck. This research was funded in part by the Austrian Science Fund (FWF) P25955 ("Origin of steppe flora and fauna in inner-Alpine dry valleys" to P.S.). Additionally, the study was funded by the Tiroler Wissenschaftsfonds TWF (project 302208 to C.M.) and the regular budget of the research group Biodiversity (https://www.uibk.ac.at/en/department-of-botany/research/biodiversity/) at the Institute of Botany of the University of Innsbruck. For open access purposes, the author has applied a CC BY public copyright license to any author accepted manuscript version arising from this submission.

Appendix A. Supplementary data

Supplementary data to this article can be found online at https://doi.org/10.1016/j.ympev.2024.108242.

References

Alexander, D.H., Novembre, J., Lange, K., 2009. Fast model-based estimation of ancestry in unrelated individuals. Genome Res. 19, 1655–1664. https://doi.org/10.1186/1471-2105-12-246.

Anderson, E., Stebbins Jr, G.L., 1954. Hybridization as an evolutionary stimulus. Evolution 378–388.

Assyov, B., Petrova, A., Dimitrov, D., Vasilev, R, 2012. Conspectus of the Bulgarian Vascular Flora. Distribution Maps and Floristic. In: Elements. Bulgarian Biodiversity Foundation, Sofia, Bulgaria.

Athanassiou, A., 2012. A skeleton of *Mammuthus trogontherii* (Proboscidea, Elephantidae) from NW Peloponnese. Greece. Quat. Int. 255, 9–28. https://doi.org/10.1016/j.quaint.2011.03.030.

Axmanová, I., Robovský, J., Tichý, L., Danihelka, J., Troeva, E., Protopopov, A., Chytrý, M., 2020. Habitats of Pleistocene megaherbivores reconstructed from the frozen fauna remains. Ecography 43, 703–713. https://doi.org/10.1111/ecog.04940.

Azani, N., Bruneau, A., Wojciechowski, M.F., Zarre, S., 2017. Molecular phylogenetics of annual *Astragalus* (Fabaceae) and its systematic implications. Bot. J. Linn. Soc. 184, 347–365. https://doi.org/10.1093/BOTLINNEAN/BOX032.

Azani, N., Bruneau, A., Wojciechowski, M.F., Zarre, S., 2019. Miocene climate change as a driving force for multiple origins of annual species in *Astragalus* (Fabaceae, Papilionoideae). Mol. Phylogenet. Evol. 137, 210–221. https://doi.org/10.1016/j.ympev.2019.05.008.

Baca, M., Popović, D., Agadzhanyan, A.K., Baca, K., Conard, N.J., Fewlass, H., Filek, T., Golubiński, M., Horáček, I., Knul, M.V., Krajcarz, M., Krokhaleva, M., Lebreton, L., Lemanik, A., Maul, L.C., Nagel, D., Noiret, P., Primault, J., Rekovets, L., Rhodes, S.E., Royer, A., Serdyuk, N.V., Soressi, M., Stewart, J.R., Strukova, T., Talamo, S., Wilczyński, J., Nadachowski, A., 2023. Ancient DNA of narrow-headed vole reveal common features of the Late Pleistocene population dynamics in cold-adapted small mammals. Proc. R. Soc. B-Biol. Sci. 290, 20222238. https://doi.org/10.1098/rspb.2022.2238.

Bădărău, A.S., Dezsi, S., Comes, O., 2000. Cercetări biogeografice asupra speciilor stepice-silvostepice de *Astragalus* L. din depresiunea Transilvaniei. Studia Universitatis Babes-Bolyai. Geographia XLV,, 2.

Bădărău, A.S., Dezsi, S., Man, T., 2001. Cercetări biogeografice asupra speciilor stepice-silvostepice de *Astragalus* L. din depresiunea Transilvaniei (II), Studia universitatis Babes-Bolyai. Geographia XLVI,, 1.

Barina, Z., 2017. Distribution atlas of vascular plants in Albania. Hungarian Natural History Museum, Budapest.

Žerdoner Čalasan, A., Hurka, H., German, D.A., Smirnov, S.V., Friesen, N., Neuffer, B., 2024. From the Iranian Plateau into the heart of the Eurasian steppe belt: The phylogeography of *Sisymbrium polymorphum* (Brassicaceae). Flora 320, 152610.

Barina, Z., Csiky, J., S., F., Jakab, G., Király, G., Lájer, K., Mesterhazy, A., Molnár V., A., J., N., Németh, C., Pál, R., Pifkó, D., Pinke, G., Schmotzer, A., Somlyay, L., Sramkó, G., R., V., Vojtkó, A., 2007. Red list of the vascular flora of Hungary. Vörös Lista. A magyarországi edényes flóra veszélyeztetett fajai.

Bartha, L., Sramkó, G., Dragoş, N., 2012. New PCR primers for partial *ycf1* amplification in *Astragalus* (Fabaceae): promising source for genus-wide phylogenies. Studia UBB Biologia 57, 33–45.

Bartha, L., Dragoş, N., Molnár, A.V., Sramkó, G., 2013. Molecular evidence for reticulate speciation in *Astragalus* (Fabaceae) as revealed by a case study from sect *Dissitiflori*. Botany 91, 702–714. https://doi.org/10.1139/cjb-2013-0036.

Becker, T., 2003. Auswirkungen langzeitiger fragmentierung auf populationen am beispiel der reliktischen steppenrasenart *Astragalus exscapus* L. (Fabaceae). Diss. Bot. 380, 1–210.

Becker, T., 2010. Explaining rarity of the dry grassland perennial *Astragalus exscapus*. Folia Geobot. 45, 303–321. https://doi.org/10.1007/S12224-010-9068-3.

Becker, T., 2013. Die Steppenreliktart *Astragalus exscapus* – eine Schlüsselart der Steppenreste Mitteleuropas? In: Baumbach, H., Pfützenreuter, S. (Eds.), Steppenlebensräume Europas – Gefährdung, Erhaltungsmaßnahmen Und Schutz.

Thüringer Ministerium für Landwirtschaft, Forsten, Umwelt und Naturschutz (TMLFUN), Erfurt, Germany, pp. 69–90.
Becker, T., Voß, N., 2003. Einnischung der seltenen Steppenrasenart *Astragalus exscapus* L. (Stengelloser Tragant) im Kyffhäusergebirge (Thüringen, Deutschland). Feddes Repert. 114, 142–165. https://doi.org/10.1002/fedr.200390000.
Binney, H., Edwards, M., Macias-Fauria, M., Lozhkin, A., Anderson, P., Kaplan, J.O., Andreev, A., Bezrukova, E., Blyakharchuk, T., Jankovska, V., 2017. Vegetation of Eurasia from the last glacial maximum to present: Key biogeographic patterns. Quat. Sci. Rev. 157, 80–97. https://doi.org/10.1016/j.quascirev.2016.11.022.
Bobo-Pinilla, J., Peñas de Giles, J., López-González, N., Mediavilla, S., Martínez-Ortega, M.M., 2018. Phylogeography of an endangered disjunct herb: Long-distance dispersal, refugia and colonization routes. AoB Plants 10. https://doi.org/10.1093/aobpla/ply047.
Bobo-Pinilla, J., López-González, N., Caballero, A., Peñas de Giles, J., 2021. Looking for a successful translocation: the case of *Astragalus edulis*. Mediterr. Bot. 42, e68048.
Bondarchuk, O.P., Rakhmetov, D.B., 2018. Evaluation of the introduction effectiveness of plants of *Astragalus* spp. in conditions of Right-Bank of Forest-Steppe of Ukraine. Інтродукція рослин 23–29.
Bouckaert, R., Vaughan, T.G., Barido-Sottani, J., Duchêne, S., Fourment, M., Gavryushkina, A., Heled, J., Jones, G., Kühnert, D., De Maio, N., 2019. BEAST 2.5: An advanced software platform for Bayesian evolutionary analysis. PLoS Comput. Biol. 15, e1006650.
Bougoutaia, Y., Garnatje, T., Vallès, J., Kaid-Harche, M., Ouhammou, A., Dahia, M., Tlili, A., Vitales, D., 2021. Phylogeographical and cytogeographical history of *Artemisia herba-alba* (Asteraceae) in the Iberian Peninsula and North Africa: mirrored intricate patterns on both sides of the Mediterranean Sea. Bot. J. Linn. Soc. 195, 588–605. https://doi.org/10.1093/BOTLINNEAN/BOAA075.
Braun-Blanquet, J., 1961. Die inneralpine Trockenvegetation. Fischer, Stuttgart, Germany.
Braun-Blanquet, J., de Bolòs, O., 1957. Les groupements végétaux du bassin moyen de l'Ebre et leur dynamisme. An. Estac. Exp. Aula Dei 5, 1–266.
Brown, W.L., 1957. Centrifugal speciation. Q. Rev. Biol. 32, 247–277. https://doi.org/10.1086/401875.
Bryant, D., Bouckaert, R., Felsenstein, J., Rosenberg, N.A., RoyChoudhury, A., 2012. Inferring species trees directly from biallelic genetic markers: bypassing gene trees in a full coalescent analysis. Mol. Biol. Evol. 29, 1917–1932. https://doi.org/10.1093/molbev/mss086.
Cai, L., Xi, Z., Lemmon, E.M., Lemmon, A.R., Mast, A., Buddenhagen, C.E., Liu, L., Davis, C.C., 2021. The perfect storm: gene tree estimation error, incomplete lineage sorting, and ancient gene flow explain the most recalcitrant ancient angiosperm clade Malpighiales. Syst. Biol. 70, 491–507. https://doi.org/10.1093/sysbio/syaa083.
Cancellieri, L., Sperandii, M.G., Filibeck, G., 2017. First record of the steppic relict *Astragalus exscapus* L. subsp. *exscapus* in the Apennines (Abruzzo, Italy), and biogeographic implications. Plant Biosyst. 151, 944–948. https://doi.org/10.1080/11263504.2017.1311963.
Casimiro-Soriguer, R., Talavera, M., Balao, F., Terrab, A., Herrera, J., Talavera, S., 2010. Phylogeny and genetic structure of *Erophaca* (Leguminosae), a East–West Mediterranean disjunct genus from the Tertiary. Mol. Phylogenet. Evol. 56, 441–450.
Catchen, J.M., Amores, A., Hohenlohe, P., Cresko, W., Postlethwait, J.H., 2011. Stacks: Building and genotyping loci de novo from short-read sequences. G3: Genes Genom Genet. 1, 171–182. https://doi.org/10.1534/G3.111.000240.
Catchen, J., Hohenlohe, P.A., Bassham, S., Amores, A., Cresko, W.A., 2013. Stacks: An analysis tool set for population genomics. Mol. Ecol. 22, 3124–3140. https://doi.org/10.1111/MEC.12354.
Chamberlain, D.F., Matthews, V.A., 1969. *Astragalus* L. In: Davis, P.H. (Ed.), Flora of Turkey and the East Aegean Islands. Edinburgh University Press, Edinburgh, UK, pp. 49–254.
Chang, D., Knapp, M., Enk, J., Lippold, S., Kircher, M., Lister, A., MacPhee, R.D., Widga, C., Czechowski, P., Sommer, R., Hodges, E., 2017. The evolutionary and phylogeographic history of woolly mammoths: a comprehensive mitogenomic analysis. Scientific Reports 7 (1), 44585.
Chen, I.-C., Hill, J.K., Ohlemüller, R., Roy, D.B., Thomas, C.D., 2011. Rapid range shifts of species associated with high levels of climate warming. Science 333, 1024–1026. https://doi.org/10.1126/science.1206432.
Chifu, T., Manzu, C., Oana, Z., 2006. Flora şi vegetatia Moldovei (Romania). I. Flora. Universitatea "Al. I. Cuza", Iaşi.
Ciocârlan, V., 2000. The romanian illustrated flora. Pteridophyta et Spermatophyta, Ceres, Bucureşti.
Ciocârlan, N., 2013. Ex situ conservation of rare medicinal plants in the Botanical Garden (Institute) of Academy of Sciences of Moldova. Acta Horti Botanici Bucurestiensis 40, 43–48. https://doi.org/10.2478/ahbb-2013-0005.
Clark, P.U., Archer, D., Pollard, D., Blum, J.D., Rial, J.A., Brovkin, V., Mix, A.C., Pisias, N. G., Roy, M., 2006. The middle Pleistocene transition: characteristics, mechanisms, and implications for long-term changes in atmospheric pCO2. Quat. Sci. Rev. 25, 3150–3184. https://doi.org/10.1016/j.quascirev.2006.07.008.
Clement, M., Posada, D., Crandall, K.A., 2000. TCS: A computer program to estimate gene genealogies. Mol. Ecol. 9, 1657–1659. https://doi.org/10.1046/j.1365-294x.2000.01020.x.
Corriveau, J.L., Coleman, A.W., 1988. Rapid screening method to detect potential biparental inheritance of plastid DNA and results for over 200 angiosperm species. Am. J. Bot. 75, 1443–1458. https://doi.org/10.1002/j.1537-2197.1988.tb11219.x.
Cremene, C., Groza, G., Rakosy, L., Schileyko, A.A., Baur, A., Erhardt, A., Baur, B., 2005. Alterations of steppe-like grasslands in Eastern Europe: a threat to regional biodiversity hotspots. Conserv. Biol. 19 (5), 1606–1618. https://doi.org/10.1111/j.1523-1739.2005.00084.x.
Danecek, P., Auton, A., Abecasis, G., Albers, C.A., Banks, E., DePristo, M.A., Handsaker, R.E., Lunter, G., Marth, G.T., Sherry, S.T., McVean, G., Durbin, R., 2011. The variant call format and VCFtools. Bioinformatics 27, 2156–2158. https://doi.org/10.1093/BIOINFORMATICS/BTR330.
De Soo, R., 1929. Die Vegetation und die Entstehung der ungarischen Puszta. J. Ecol. 17, 329–350.
Dengler, J., Janišová, M., Török, P., Wellstein, C., 2014. Biodiversity of Palaearctic grasslands: a synthesis. Agr Ecosyst Environ 182, 1–14. https://doi.org/10.1016/j.agee.2013.12.015.
Dengler, J., Biurrun, I., Boch, S., Dembicz, I., Török, P., 2020. Grasslands of the palaearctic biogeographic realm: introduction and synthesis. Encyclopedia of the World's Biomes 3, 617–637. https://doi.org/10.1016/B978-0-12-409548-9.12432-7.
Díaz, S., Lavorel, S., Mcintyre, S., Falczuk, V., Casanoves, F., Milchunas, D.G., Skarpe, C., Rusch, G., Sternberg, M., Noy-Meir, I., Landsberg, J., Zhang, W., Clark, H., Campbell, B.D., 2007. Plant trait responses to grazing – a global synthesis. Glob. Change Biol. 13, 313–341. https://doi.org/10.1111/j.1365-2486.2006.01288.x.
Diklić, N., 1972. *Astragalus* L. – pp. 274-301 in: Josifović, M. (Ed.): Flora SR Srbije, 4. Beograd.
Doležel, J., Greilhuber, J., Suda, J., 2007. Estimation of nuclear DNA content in plants using flow cytometry. Nat. Protoc. 2, 2233–2244. https://doi.org/10.1038/nprot.2007.310.
Durand, E.Y., Patterson, N., Reich, D., Slatkin, M., 2011. Testing for ancient admixture between closely related populations. Mol. Biol. Evol. 28, 2239–2252. https://doi.org/10.1093/molbev/msr048.
Dvořák, F., Dadáková, B., Grüll, F., 1977. Studies of the morphology of chromosomes of some selected species. Folia Geobot. Phytotax. 12, 343–375. https://doi.org/10.1007/BF02890649.
Earl, D.A., vonHoldt, B.M., 2012. Structure harvester: a website and program for visualizing structure output and implementing the Evanno method. Conserv. Genet. Resour. 4, 359–361. https://doi.org/10.1007/s12686-011-9548-7.
Egorov, A.V., Zernov, A.S., Onipchenko, V.G., 2020. North-Western Caucasus, in: Noroozi, J. (Ed.), Plant biogeography and vegetation of high mountains of Central and South-West Asia. Springer, Cham, Switzerland, pp. 315–360. doi: 10.1007/978-3-030-45212-4_9.
Ellenberg, H., Leuschner, C., 2010. Vegetation Mitteleuropas mit den Alpen: In ökologischer, dynamischer und historischer Sicht. UTB. ISBN: 9783825281045.
Evanno, G., Regnaut, S., Goudet, J., 2005. Detecting the number of clusters of individuals using the software structure: a simulation study. Mol. Ecol. 14, 2611–2620. https://doi.org/10.1111/j.1365-294X.2005.02553.x.
Falush, D., Stephens, M., Pritchard, J.K., 2003. Inference of population structure using multilocus genotype data: linked loci and correlated allele frequencies. Genetics 164, 1567–1587. https://doi.org/10.1093/genetics/164.4.1567.
Fedorov, A.A., Bobrov, A.E., Tsvelëv, N.N., 2002. Flora of Russia - Volume 6. Oxford & IBH Publishing Company Pvt, Limited.
Feoktistova, N.Y., Meschersky, I.G., Bogomolov, P.L., Sayan, A.S., Poplavskaya, N.S., Surov, A.V., 2017. Phylogeographic structure of the Common hamster (*Cricetus cricetus* L.): Late Pleistocene connections between Caucasus and Western European populations. PLoS One 12, e0187527.
Ferrández Palacio, J.V., 2003. *Astragalus exscapus* L. (Leguminosae), nueva especie para la flora de la Península Ibérica. Collect. Bot. (barcelona) 26, 119–124. https://doi.org/10.3989/collectbot.2003.v26.18.
Feurdean, A., Ruprecht, E., Molnár, Z., Hutchinson, S.M., Hickler, T., 2018. Biodiversity-rich European grasslands: Ancient, forgotten ecosystems. Biol. Conserv. 228, 224–232. https://doi.org/10.1016/j.biocon.2018.09.022.
Fischer, M.A., Oswald, K., Adler, W., 2008. Exkursionsflora für Österreich, Liechtenstein und Südtirol, 3. Aufl. Biologiezentrum der Oberösterreichischen Landesmuseen, Linz.
Fleming, J.F., Valero-Gracia, A., Struck, T.H., 2023. Identifying and addressing methodological incongruence in phylogenomics: A review. Evol. Appl. 16, 1087–1104. https://doi.org/10.1111/eva.13565.
Folk, R.A., Visger, C.J., Soltis, P.S., Soltis, D.E., Guralnick, R.P., 2018. Geographic range dynamics drove ancient hybridization in a lineage of angiosperms. Am. Nat. 192, 171–187. https://doi.org/10.1086/698120.
Folk, R.A., Gaynor, M.L., Engle-Wrye, N.J., O'Meara, B.C., Soltis, P.S., Soltis, D.E., Guralnick, R.P., Smith, S.A., Grady, C.J., Okuyama, Y., 2023. Identifying climatic drivers of hybridization with a new ancestral niche reconstruction method. Syst. Biol. 72, 856–873.
Folk, R.A., Maassoumi, A.A., Siniscalchi, C.M., Kates, H.R., Soltis, D.E., Soltis, P.S., Belitz, M.B., Guralnick, R.P., 2024a. Phylogenetic diversity and regionalization in the temperate arid zone. J. Syst. Evol. jse.13077. https://doi.org/10.1111/jse.13077.
Folk, R.A., Charboneau, J.L.M., Belitz, M., Singh, T., Kates, H.R., Soltis, D.E., Soltis, P.S., Guralnick, R.P., Siniscalchi, C.M., 2024b. Anatomy of a mega-radiation: Biogeography and niche evolution in *Astragalus*. Am. J. Bot. 111, e16299.
Fougrach, H., Badri, W., Malki, M., 2007. Flore vasculaire rare et menacée du massif de Tazekka (région de Taza, Maroc). Bulletin De L'institut Scientifique, Rabat, Section Sciences De La Vie 29, 1–10.
Frajman, B., Schönswetter, P., 2011. Giants and dwarfs: Molecular phylogenies reveal multiple origins of annual spurges within *Euphorbia* subg *Esula*. Mol. Phylogenet. Evol. 61, 413–424. https://doi.org/10.1016/J.YMPEV.2011.06.011.
Frajman, B., Záveská, E., Gamisch, A., Moser, T., Arthofer, W., Hilpold, A., Kirschner, P., Paun, O., Sanmartin, I., Schlick-Steiner, B.C., Schönswetter, P., Steiner, F.M., Trucchi, E., 2019. Integrating phylogenomics, phylogenetics, morphometrics,

relative genome size and ecological niche modelling disentangles the diversification of Eurasian *Euphorbia seguieriana* s. l. (Euphorbiaceae). Mol. Phylogenet. Evol. 134, 238–252. https://doi.org/10.1016/j.ympev.2018.10.046.
Ghasemi, A., Hemami, M.R., Karimi, S., Iravani, M., Senn, J., 2024. Potential seed dispersal by persian wild ass in south central Iran. Rangel. Ecol. Manage. 92, 73–79.
Gil-López, M.J., Segarra-Moragues, J.G., Casimiro-Soriguer, R., Ojeda, F., 2022. From the Strait of Gibraltar to northern Europe: Pleistocene refugia and biogeographic history of heather (*Calluna vulgaris*, Ericaceae). Bot. J. Linn. Soc. 198, 41–56. https://doi.org/10.1093/botlinnean/boab043.
Goncharov, N. F., Borisova, A. G., Gorshkova, S. G., Popov, M. G., Vasilchenko, I. T., 1946: *Astragalus*. In: Komarov V. L., Shishkin, B. K. (Eds.): Flora of the U.S.S.R. Vol. XII. Leguminosae: *Astragalus*. Israel Program for Scientific Translations, Jerusalem, Smithsonian Institution and the National Science Foundation, Washington, D.C. 1965, pp. 1–918 (translated by Landau, N.; Russian Original: Izdatel'stvo Akademii Nauk SSSR, Moskow, Leningrad 1946).
Green, R.E., Krause, J., Briggs, A.W., Maricic, T., Stenzel, U., Kircher, M., Patterson, N., Li, H., Zhai, W., Fritz, M.-H.-Y., Hansen, N.F., Durand, E.Y., Malaspinas, A.-S., Jensen, J.D., Marques-Bonet, T., Alkan, C., Prüfer, K., Meyer, M., Burbano, H.A., Good, J.M., Schultz, R., Aximu-Petri, A., Butthof, A., Höber, B., Höffner, B., Siegemund, M., Weihmann, A., Nusbaum, C., Lander, E.S., Russ, C., Novod, N., Affourtit, J., Egholm, M., Verna, C., Rudan, P., Brajkovic, D., Kucan, Ž., Gušic, I., Doronichev, V.B., Golovanova, L.V., Lalueza-Fox, C., De La Rasilla, M., Fortea, J., Rosas, A., Schmitz, R.W., Johnson, P.L.F., Eichler, E.E., Falush, D., Birney, E., Mullikin, J.C., Slatkin, M., Nielsen, R., Kelso, J., Lachmann, M., Reich, D., Pääbo, S., 2010. A draft sequence of the neandertal genome. Science 328, 710–722. https://doi.org/10.1126/science.1188021.
Guzmán, B., Vargas, P., 2009. Long-distance colonization of the Western Mediterranean by *Cistus ladanifer* (Cistaceae) despite the absence of special dispersal mechanisms. J. Biogeogr. 36, 954–968. https://doi.org/10.1111/j.1365-2699.2008.02040.x.
Hall, T.A., 1999. BioEdit: A user-friendly biological sequence alignment editor and analysis program for Windows 95/98/NT. Nucleic Acids Symp. Ser. 41, 95–98.
Hardion, L., Dumas, P.J., Abdel-Samad, F., Bou Dagher Kharrat, M., Surina, B., Affre, L., Médail, F., Bacchetta, G., Baumel, A., 2016. Geographical isolation caused the diversification of the Mediterranean thorny cushion-like *Astragalus* L. sect. *Tragacantha* DC. (Fabaceae). Mol. Phylogenet. Evol. 97, 187–195. https://doi.org/10.1016/j.ympev.2016.01.006.
Hays, J.D., Imbrie, J., Shackleton, N.J., 1976. Variations in the Earth's Orbit: Pacemaker of the Ice Ages: For 500,000 years, major climatic changes have followed variations in obliquity and precession. Science 194, 1121–1132. https://doi.org/10.1126/science.194.4270.1121.
Heled, J., Drummond, A.J., 2015. Calibrated birth–death phylogenetic time-tree priors for Bayesian inference. Syst. Biol. 64, 369–383. https://doi.org/10.1093/sysbio/syu089.
Herbert, T.D., 2023. The Mid-Pleistocene Climate Transition. Annu. Rev. Earth Planet. Sci. 51, 389–418. https://doi.org/10.1146/annurev-earth-032320-104209.
Herrando-Moraira, S., Roquet, C., Calleja, J.-A., Chen, Y.-S., Fujikawa, K., Galbany-Casals, M., Garcia-Jacas, N., Liu, J.-Q., López-Alvarado, J., López-Pujol, J., Mandel, J.R., Mehregan, I., Sáez, L., Sennikov, A.N., Susanna, A., Vilatersana, R., Xu, L.-S., 2023. Impact of the climatic changes in the Pliocene-Pleistocene transition on Irano-Turanian species. The radiation of genus *Jurinea* (Compositae). Mol. Phylogenet. Evol. 189, 107928. https://doi.org/10.1016/j.ympev.2023.107928.
Hewitt, G.M., 2011. Quaternary phylogeography: the roots of hybrid zones. Genetica 139, 617–638. https://doi.org/10.1007/s10709-011-9547-3.
Hodková, E., Doudová, J., Douda, J., Krak, K., Mandák, B., 2019. On the road: Postglacial history and recent expansion of the annual *Atriplex tatarica* in Europe. J. Biogeogr. 46, 2609–2621. https://doi.org/10.1111/jbi.13687.
Holmgren, P.K., 1990. Index Herbariorum: Part 1: the Herbaria of the World. International Association for Plant Taxonomy / New York Botanical Garden.
Houghton, S., Stevens, M.T., Meyer, S.E., 2020. Pods as sails but not as boats: Dispersal ecology of a habitat-restricted desert milkvetch. Am. J. Bot. 107 (6), 864–875.
Hühn, P., Dillenberger, M.S., Gerschwitz-Eidt, M., Hörandl, E., Los, J.A., Messerschmid, T.F.E., Paetzold, C., Rieger, B., Kadereit, G., 2022. How challenging RADseq data turned out to favor coalescent-based species tree inference. A case study in *Aichryson* (Crassulaceae). Mol. Phylogenet. Evol. 167, 107342. https://doi.org/10.1016/j.ympev.2021.107342.
Hurka, H., Friesen, N., Bernhardt, K.G., Neuffer, B., Smirnov, S.V., Shmakov, A.I., Blattner, F.R., 2019. The Eurasian steppe belt: Status quo, origin and evolutionary history. Turczaninowia 22, 5–71. https://doi.org/10.14258/turczaninowia.22.3.1.
Huson, D.H., Bryant, D., 2005. Application of phylogenetic networks in evolutionary studies. Mol. Biol. Evol. 23, 254–267. https://doi.org/10.1093/molbev/msj030.
Iriondo, J. M., Albert, M. J., Giménez Benavides, L., Domínguez Lozano, F., Escudero, A. (Eds.) 2009. Poblaciones en Peligro: Viabilidad Demográfica de la Flora Vascular Amenazada de España. Dirección General de Medio Natural y Política Forestal (Ministerio de Medio Ambiente, y Medio Rural y Marino), Madrid, pp. 242.
Jaganathan, G.K., Li, J., Biddick, M., Han, K., Song, D., Yang, Y., Han, Y., Liu, B., 2019. Mechanisms underpinning the onset of seed coat impermeability and dormancy-break in *Astragalus adsurgens*. Sci. Rep. 9 (1), 9695.
Jäger, E.J., 1971. Die pflanzengeographische Stellung der „Steppen" der Iberischen Halbinsel. Flora 160, 217–256. https://doi.org/10.1016/S0367-2530(17)31669-9.
Jakobsson, M., Rosenberg, N.A., 2007. CLUMPP: a cluster matching and permutation program for dealing with label switching and multimodality in analysis of population structure. Bioinformatics 23, 1801–1806. https://doi.org/10.1093/bioinformatics/btm233.
Jännicke, W., 1892. Die Sandflora von Mainz: Ein Relict aus der Steppenzeit. Gebr, Knauer.
Javanmardi, F., Kazempour Osaloo, S., Maassoumi, A.A., Nejadsattrai, T., 2012. Molecular phylogeny of *Astragalus* section *Alopecuroidei* (Fabaceae) and its allies based on nrDNA ITS and three cpDNAs, matK, trnT-trnY and trnH-psbA sequences. Biochem. Syst. Ecol. 45, 171–178. https://doi.org/10.1016/j.bse.2012.07.029.
Kahlke, R.D., García, N., Kostopoulos, D.S., Lacombat, F., Lister, A.M., Mazza, P.P.A., Spassov, N., Titov, V.V., 2011. Western Palaearctic palaeoenvironmental conditions during the Early and early Middle Pleistocene inferred from large mammal communities, and implications for hominin dispersal in Europe. Quat. Sci. Rev. 30, 1368–1395. https://doi.org/10.1016/J.QUASCIREV.2010.07.020.
Kahlke, R.D., 2014. The origin of Eurasian Mammoth Faunas (*Mammuthus–Coelodonta* Faunal Complex). Quat. Sci. Rev., Predators, Prey and Hominins - Celebrating the Scientific Career of Alan Turner (1947-2012) 96, 32–49. https://doi.org/10.1016/j.quascirev.2013.01.012.
Kajtoch, Ł., Cieślak, E., Varga, Z., Paul, W., Mazur, M.A., Sramkó, G., Kubisz, D., 2016. Phylogeographic patterns of steppe species in Eastern Central Europe: A review and the implications for conservation. Biodivers. Conserv. 25, 2309–2339. https://doi.org/10.1007/S10531-016-1065-2.
Kalyaanamoorthy, S., Minh, B.Q., Wong, T.K.F., von Haeseler, A., Jermiin, L.S., 2017. ModelFinder: Fast model selection for accurate phylogenetic estimates. Nat. Methods 14, 587–589. https://doi.org/10.1038/nmeth.4285.
Kamp, J., Koshkin, M.A., Bragina, T.M., Katzner, T.E., Milner-Gulland, E.J., Schreiber, D., Sheldon, R., Shmalenko, A., Smelansky, I., Terraube, J., Urazaliev, R., 2016. Persistent and novel threats to the biodiversity of Kazakhstan's steppes and semi-deserts. Biodivers. Conserv. 25, 2521–2541.
Kazemi, M., Kazempour Osaloo, S., Maassoumi, A.A., Pouyani, E.R., 2009. Molecular phylogeny of selected Old World *Astragalus* (Fabaceae): Incongruence among chloroplast *trnL-F*, *ndhF* and nuclear ribosomal DNA ITS sequences. Nord. J. Bot. 27, 425–436. https://doi.org/10.1111/J.1756-1051.2009.00285.X.
Kazempour Osaloo, S., Maassoumi, A.A., Murakami, N., 2003. Molecular systematics of the genus *Astragalus* L. (Fabaceae): Phylogenetic analyses of nuclear ribosomal DNA internal transcribed spacers and chloroplast gene *ndh*F sequences. Plant Syst. Evol. 242, 1–32. https://doi.org/10.1007/s00606-003-0014-1.
Kazempour Osaloo, S., Maassoumi, A.A., Murakami, N., 2005. Molecular systematics of the Old World *Astragalus* (Fabaceae) as inferred from nrDNA ITS sequence data. Brittonia 57, 367–381. https://doi.org/10.1663/0007-196X(2005)057[0367:MSOTOW]2.0.CO;2.
Kienberg, O., Becker, T., 2017. Differences in population structure require habitat-specific conservation strategies in the threatened steppe grassland plant *Astragalus exscapus*. Biol. Conserv. 211, 56–66. https://doi.org/10.1016/J.BIOCON.2017.05.002.
Kimura, M., 1980. A simple method for estimating evolutionary rates of base substitutions through comparative studies of nucleotide sequences. J. Mol. Evol. 16, 111–120. https://doi.org/10.1007/BF01731581.
Kirschner, P., Záveská, E., Gamisch, A., Hilpold, A., Trucchi, E., Paun, O., Sanmartín, I., Schlick-Steiner, B.C., Frajman, B., Arthofer The STEPPE Consortium, W., Steiner, F. M., Schönswetter, P., 2020. Long-term isolation of European steppe outposts boosts the biome's conservation value. Nat. Commun. 11, 1968. https://doi.org/10.1038/s41467-020-15620-2.
Kirschner, P., Perez, M.F., Záveská, E., Sanmartín, I., Marquer, L., Schlick-Steiner, B.C., Alvarez, N., the STEPPE Consortium, Steiner, F.M., Schönswetter, P., 2022. Congruent evolutionary responses of European steppe biota to late Quaternary climate change. Nat. Commun. 13, 1921. https://doi.org/10.1038/s41467-022-29267-8.
Kirschner, P., Seifert, B., Kröll, J., the STEPPE Consortium, Schlick-Steiner, B.C., Steiner, F.M., 2023. Phylogenomic inference and demographic model selection suggest peripatric separation of the cryptic steppe ant species *Plagiolepis pyrenaica* stat. rev. Mol. Ecol. 32, 1149–1168. https://doi.org/10.1111/mec.16828.
Kryštufek, B., Bryja, J., Bužan, E.V., 2009. Mitochondrial phylogeography of the European ground squirrel, *Spermophilus citellus*, yields evidence on refugia for steppic taxa in the southern Balkans. Hered. 103, 129–135. https://doi.org/10.1038/hdy.2009.41.
Kukuła, K., Okarma, H., Pawłowski, J., Perzanowski, K., Ruzicka, T., Sandor, J., Stanova, V., Tasenkevich, L., Vlasin, M., 2003. Carpathian List of Endangered Species; WWF International Danube-Carpathian Programme: Vienna, Austria; Institute of Nature Conservation, Polish Academy of Sciences: Krakow, Poland, 2003; pp. 1–64. ISBN 83–918914–0–2.
Laczkó, L., Jordán, S., Sramkó, G., 2022. The RadOrgMiner pipeline: Automated genotyping of organellar loci from RADseq data. Methods Ecol. Evol. 13, 1962–1975. https://doi.org/10.1111/2041-210X.13937.
Lavin, M., Herendeen, P.S., Wojciechowski, M.F., 2005. Evolutionary rates analysis of Leguminosae implicates a rapid diversification of lineages during the Tertiary. Syst. Biol. 54, 575–594. https://doi.org/10.1080/10635150590947131.
Leaché, A.D., Banbury, B.L., Felsenstein, J., De Oca, A.N.M., Stamatakis, A., 2015. Short tree, long tree, right tree, wrong tree: New acquisition bias corrections for inferring SNP phylogenies. Syst. Biol. 64, 1032–1047. https://doi.org/10.1093/SYSBIO/SYV053.
Leigh, J.W., Bryant, D., 2015. POPART: Full-feature software for haplotype network construction. Methods Ecol. Evol. 6, 1110–1116. https://doi.org/10.1111/2041-210X.12410.
Lisiecki, L.E., Raymo, M.E., 2007. Plio–Pleistocene climate evolution: trends and transitions in glacial cycle dynamics. Quat. Sci. Rev. 26, 56–69. https://doi.org/10.1016/j.quascirev.2006.09.005.
Loidi, J. (Ed.), 2017. The Vegetation of the Iberian Peninsula. Plant and Vegetation. Springer, Cham, 10.1007/978-3-319-54784-8.

Lorite, J., Navarro, F.B., Valle, F., 2007. Estimation of threatened orophytic flora and priority of its conservation in the Baetic range (S. Spain). Plant Biosyst. 141, 1–14. https://doi.org/10.1080/11263500601153560.
Lovas-Kiss, Á., Sonkoly, J., Vincze, O., Green, A.J., Takács, A., Molnár, A.V., 2015. Strong potential for endozoochory by waterfowl in a rare, ephemeral wetland plant species, *Astragalus contortuplicatus* (Fabaceae). Acta Soc. Bot. Pol. 84 (3).
Maassoumi, A.A., 1989. Notes on the genus *Astragalus* in Iran IV, Cytotaxonomic studies on some species (Dedicated to Prof. Dr. E. Esfandiari on the occasion of his 80th birthday). Iran. J. Bot. 4, 153–163.
Maassoumi, A.A., Ashouri, P., 2022. The hotspots and conservation gaps of the mega genus *Astragalus* (Fabaceae) in the Old-World. Biodivers. Conserv. 31, 2119–2139. https://doi.org/10.1007/s10531-022-02429-2.
Maddison, W. P., Maddison D.R., 2023. Mesquite: a modular system for evolutionary analysis.
Magnes, M., Willner, W., Janišová, M., Mayrhofer, H., Afif Khouri, E., 2021. Xeric grasslands of the inner-alpine dry valleys of Austria–new insights into syntaxonomy, diversity and ecology. Veg. Classif. Surv. 2, 133–157. https://doi.org/10.3897/VCS/2021/68594.
Magyari, E.K., Chapman, J.C., Gaydarska, B., Marinova, E., Deli, T., Huntley, J.P., Allen, J.R.M., Huntley, B., 2008. The 'oriental' component of the Balkan flora: evidence of presence on the Thracian Plain during the Weichselian late-glacial. J. Biogeogr. 35, 865–883. https://doi.org/10.1111/j.1365-2699.2007.01849.x.
Magyari, E.K., Chapman, J.C., Passmore, D.G., Allen, J.R.M., Huntley, J.P., Huntley, B., 2010. Holocene persistence of wooded steppe in the Great Hungarian Plain. J. Biogeogr. 37, 915–935. https://doi.org/10.1111/J.1365-2699.2009.02261.X.
Malinsky, M., Svardal, H., Tyers, A.M., Miska, E.A., Genner, M.J., Turner, G.F., Durbin, R., 2018. Whole-genome sequences of Malawi cichlids reveal multiple radiations interconnected by gene flow. Nat. Ecol. Evol. 2, 1940–1955.
Malinsky, M., Matschiner, M., Svardal, H., 2021. Dsuite - Fast *D* -statistics and related admixture evidence from VCF files. Mol. Ecol. Resour. 21, 584–595. https://doi.org/10.1111/1755-0998.13265.
Mallet, J., 2005. Hybridization as an invasion of the genome. Trends Ecol. Evol. 20, 229–237. https://doi.org/10.1016/J.TREE.2005.02.010.
Mallet, J., Besansky, N., Hahn, M.W., 2016. How reticulated are species? Bioessays 38, 140–149. https://doi.org/10.1002/bies.201500149.
Manafzadeh, S., Staedler, Y.M., Conti, E., 2017. Visions of the past and dreams of the future in the Orient: The Irano-Turanian region from classical botany to evolutionary studies. Biol. Rev. Camb. Philos. Soc. 92, 1365–1388. https://doi.org/10.1111/brv.12287.
Martin, S.H., Davey, J.W., Jiggins, C.D., 2015. Evaluating the use of ABBA–BABA statistics to locate introgressed loci. Mol. Biol. Evol. 32, 244–257. https://doi.org/10.1093/molbev/msu269.
Martin, E., Duran, A., Dinç, M., Erişen, S., Babaoğlu, M., 2008. Karyotype analyses of four *Astragalus* L. (Fabaceae) species from Turkey. Phytologia 90, 147–159.
Martín-Rodríguez, I., Vargas, P., Ojeda, F., Fernández-Mazuecos, M., 2020. An enigmatic carnivorous plant: ancient divergence of Drosophyllaceae but recent differentiation of *Drosophyllum lusitanicum* across the Strait of Gibraltar. Syst. Biodivers. 18, 525–537. https://doi.org/10.1080/14772000.2020.1771467.
Matzke, N.J., 2013. Probabilistic historical biogeography: new models for founder-event speciation, imperfect detection, and fossils allow improved accuracy and model-testing. University of California, Berkeley.
Matzke, N.J., 2014. Model selection in historical biogeography reveals that founder-event speciation is a crucial process in island clades. Syst. Biol. 63, 951–970. https://doi.org/10.1093/sysbio/syu056.
Maylandt, C., Seidl, A., Kirschner, P., Pfanzelt, S., Király, G., Neuffer, B., Blattner, F.R., Hurka, H., Friesen, N., Poluyanov, A.V., 2024. Phylogeography of the Euro-Siberian steppe plant *Astragalus austriacus*: Late Pleistocene climate fluctuations fuelled formation and expansion of two main lineages from a Pontic-Pannonian area of origin. Perspect. Plant Ecol. Evol. Syst. 125800. https://doi.org/10.1016/j.ppees.2024.125800.
Meirmans, P.G., 2018. Subsampling reveals that unbalanced sampling affects Structure results in a multi-species dataset. Hered. 122, 276–287. https://doi.org/10.1038/s41437-018-0124-8.
Mesícek, J., Javurková-Jarolímová, V., 1992. List of chromosome numbers of the Czech vascular plants. Academia, Praha.
Meusel, H., Jäger, E., Weinert, E., 1965. Vergleichende Chorologie der zentraleuropäischen Flora. Fischer, Jena, Deutschland.
Migliore, J., Baumel, A., Juin, M., Médail, F., 2012. From Mediterranean shores to central Saharan mountains: key phylogeographical insights from the genus *Myrtus*. J. Biogeogr. 39, 942–956. https://doi.org/10.1111/j.1365-2699.2011.02646.x.
Molnár, Zs., Biró, M., Bartha, S., Fekete, G., 2012. Past Trends, Present State and Future Prospects of Hungarian Forest-Steppes. In J. A. M. Werger and M. A. van Staalduinen (Eds.), Eurasian steppes. Ecological problems and livelihoods in a changing world, Springer. pp. 209–252. doi: 10.1007/978-94-007-3886-7_7.
Mosyakin, S., Fedoronchuk, M., 1999. Vascular plants of Ukraine. A nomenclatural checklist. Institute of Botany, Kyiv, pp. 206–208.
Mucina, L., Grabherr, G., Ellmauer, T., 1993. Die Pflanzengesellschaften Österreichs. Teil I. Gustav Fischer Verlag, Jena. 578 pp., ISBN 3-334-60452-7.
Nathan, R., 2006. Long-distance dispersal of plants. Science 313, 786–788. https://doi.org/10.1126/science.1124975.
Nei, M., 1972. Genetic distance between populations. Am. Nat. 106, 283–292. https://doi.org/10.1086/282771.
Nieto Feliner, G., 2014. Patterns and processes in plant phylogeography in the Mediterranean Basin. A review. Perspect. Plant Ecol. Evol. Syst. 16, 265–278.
Ortiz, E.M., 2019. vcf2phylip v2.0: convert a VCF matrix into several matrix formats for phylogenetic analysis. https://doi.org/105281/zenodo 2540861.
Ottenburghs, J., Megens, H.-J., Kraus, R.H.S., van Hooft, P., van Wieren, S.E., Crooijmans, R.P.M.A., Ydenberg, R.C., Groenen, M.A.M., Prins, H.H.T., 2017. A history of hybrids? Genomic patterns of introgression in the True Geese. BMC Evol. Biol. 17, 201. https://doi.org/10.1186/s12862-017-1048-2.
Palkopoulou, E., Dalén, L., Lister, A.M., Vartanyan, S., Sablin, M., Sher, A., Nyström Edmark, V., Brandström, M.D., Germonpré, M., Barnes, I., Thomas, J.A., 2013. Holarctic genetic structure and range dynamics in the woolly mammoth. Proc. R. Soc. Lond. B: Biol. Sci. 280, 20131910. https://doi.org/10.1098/rspb.2013.1910.
Paris, J.R., Stevens, J.R., Catchen, J.M., 2017. Lost in parameter space: a road map for stacks. Methods Ecol. Evol. 8, 1360–1373. https://doi.org/10.1111/2041-210X.12775.
Parnikoza, I., Vasiluk, A., 2011. Ukrainian steppes: current state and perspectives for protection. In Annales Universitatis Mariae Curie-Sklodowska (Vol. 66, No. 1, p. 23). Maria Curie-Skłodowska University.
Pattengale, N.D., Alipour, M., Bininda-Emonds, O.R.P., Moret, B.M.E., Stamatakis, A., 2010. How many bootstrap replicates are necessary? J. Comput. Biol. 17, 337–354. https://doi.org/10.1089/CMB.2009.0179.
Patterson, N., Moorjani, P., Luo, Y., Mallick, S., Rohland, N., Zhan, Y., Genschoreck, T., Webster, T., Reich, D., 2012. Ancient admixture in human history. Genetics 192, 1065–1093. https://doi.org/10.1534/genetics.112.145037.
Paun, O., Turner, B., Trucchi, E., Munzinger, J., Chase, M.W., Samuel, R., 2016. Processes driving the adaptive radiation of a tropical tree (*Diospyros*, Ebenaceae) in new caledonia, a biodiversity hotspot. Syst. Biol. 65, 212–227. https://doi.org/10.1093/SYSBIO/SYV076.
Pavlova, D., 1988. Karyological study of several species from g. *Astragalus* L. Dokl. Bulg. Acad. Nauk. 67–69.
Pavlova, D., Tosheva, A., 2002a. Reports (1284-1287). – In: Kamari, G. and al. (eds), Mediterranean chromosome number reports – 12. – Fl. Medit., 12, 450-454.
Pellicer, J., Hidalgo, O., Dodsworth, S., Leitch, I.J., 2018. Genome size diversity and its impact on the evolution of land plants. Genes 9, 88. https://doi.org/10.3390/genes9020088.
Pembleton, L.W., Cogan, N.O.I., Forster, J.W., 2013. StAMPP: an R package for calculation of genetic differentiation and structure of mixed-ploidy level populations. Mol. Ecol. Resour. 13, 946–952. https://doi.org/10.1111/1755-0998.12129.
Petit, R.J., Bodénès, C., Ducousso, A., Roussel, G., Kremer, A., 2004. Hybridization as a mechanism of invasion in oaks. New Phytol. 161, 151–164. https://doi.org/10.1046/j.1469-8137.2003.00944.x.
Petrova, A., Vladimirov, V., 2009. Red List of Bulgarian vascular plants. Phytol. Balc. 15, 63–94.
Petrova, A., Vladimirov, V., 2020. Chromosome atlas of the Bulgarian vascular plants. Phytol. Balc. 26, 217–427.
Pils, G., 2016. Illustrated Flora of Albania. Gerhard Pils Verlag.
Podlech, D., 1986. Taxonomic and phytogeographical problems in *Astragalus* of the Old World and South-West Asia. Proc. R. Soc. Edin. B: Biol. Sci. 89, 37–43.
Podlech, D., 1988. Revision von *Astragalus* L. sect. *Caprini* DC. (Leguminosae). Mitt. Bot. Staatssamml. München 25, 1–924.
Podlech, D., 2011. Thesaurus Astragalorum: Index of all taxa within the genus *Astragalus* L. and other genera but belonging to the genus *Astragalus*. Taxa of the Old World and Related Taxa of the New World.
Podlech, D., Zarre, Sh., 2013. A taxonomic revision of the genus *Astragalus* L. (Leguminosae) in the Old World. Natural History Museum, Vienna, Austria.
Podlech, D., 1999. Papilionaceae III. In: Rechinger, K. H. (Ed.). Flora Iranica. Vol. 174. Akademische Druck und Verlagsanstalt, Wien, Austria, pp. 154–335.
Popescu, S.M., Biltekin, D., Winter, H., Suc, J.P., Melinte-Dobrinescu, M.C., Klotz, S., Rabineau, M., Combourieu-Nebout, N., Clauzon, G., Deaconu, F., 2010. Pliocene and lower pleistocene vegetation and climate changes at the european scale: long pollen records and climatostratigraphy. Quat. Int. 219, 152–167. https://doi.org/10.1016/j.quaint.2010.03.013.
Pritchard, J.K., Stephens, M., Donnelly, P., 2000. Inference of population structure using multilocus genotype data. Genetics 155, 945–959. https://doi.org/10.1093/genetics/155.2.945.
Pross, J., Koutsodendris, A., Christanis, K., Fischer, T., Fletcher, W.J., Hardiman, M., Kalaitzidis, S., Knipping, M., Kotthoff, U., Milner, A.M., 2015. The 1.35-Ma-long terrestrial climate archive of Tenaghi Philippon, northeastern Greece: Evolution, exploration, and perspectives for future research. Newsl. Stratigr. 48, 253–276.
Puechmaille, S.J., 2016. The program structure does not reliably recover the correct population structure when sampling is uneven: subsampling and new estimators alleviate the problem. Mol. Ecol. Resour. 16, 608–627. https://doi.org/10.1111/1755-0998.12512.
Qosja, Xh., Paparisto, K., Demiri, M., Vangjeli, J., Balza, E., 1992. Flore de l'Albanie (Flora e Shqiperise). Vol. 2. Akademia e Shkencave e Republikes se Shqiperise Qendra e Kerkimeve Biologjike, Tiranë.
Rambaut, A., Drummond, A.J., Xie, D., Baele, G., Suchard, M.A., 2018. Posterior summarization in Bayesian phylogenetics using Tracer 1.7. Syst. Biol. 67, 901–904.
Rambaut, A., 2016. FigTree v1.4.4. Available from: http://tree.bio.ed.ac.uk/software/figtree/.
Ramos-Gutiérrez, I., Moreno-Saiz, J.C., Fernández-Mazuecos, M., 2022. A western representative of an eastern clade: Phylogeographic history of the gypsum-associated plant *Nepeta hispanica*. Perspect. Plant Ecol. Evol. Syst. 57, 125699. https://doi.org/10.1016/j.ppees.2022.125699.
Riahi, M., Zarre, S., Maassoumi, A.A., Osaloo, S.K., Wojciechowski, M.F., 2011. Towards a phylogeny for *Astragalus* section *Caprini* (Fabaceae) and its allies based on nuclear and plastid DNA sequences. Plant Syst. Evol. 293, 119–133. https://doi.org/10.1007/s00606-011-0417-3.

Rieseberg, L.H., Soltis, D.E., 1991. Phylogenetic consequences of cytoplasmic gene flow in plants. Evol. Trends Plants 5, 65–84.
Romo, A.M., 2002. *Astragalus* L. In: Valdés, B., Rejdali, M., Achhal El Kadmiri, A., Jury, J. L., Montserrat, J.M. (Eds.) Catalogue des plantes vasculaires du nord du Maroc, incluant des clés d'identification, vol. 1. Biblioteca de Ciencias, CSIC, Madrid, pp. 392–398.
Rose, J.P., Toledo, C.A.P., Lemmon, E.M., Lemmon, A.R., Sytsma, K.J., 2021. Out of sight, out of mind: widespread nuclear and plastid-nuclear discordance in the flowering plant genus *Polemonium* (Polemoniaceae) suggests widespread historical gene flow despite limited nuclear signal. Syst. Biol. 70, 162–180. https://doi.org/10.1093/sysbio/syaa049.
Rumpf, S.B., Hülber, K., Klonner, G., Moser, D., Schütz, M., Wessely, J., Willner, W., Zimmermann, N.E., Dullinger, S., 2018. Range dynamics of mountain plants decrease with elevation. Proc. Natl. Acad. Sci. 115, 1848–1853. https://doi.org/10.1073/pnas.1713936115.
Sánchez-Gómez, P., M.A. Carrión, A. Hernández. 2004. *Astragalus cavanillesii* Pau, in: Bañares Á., Blanca G., Güemes J., Moreno J.C., Ortiz S., eds. 2004. Atlas y Libro Rojo de la Flora Vascular Amenazada de España. Dirección General de Conservación de la Naturaleza. Madrid, pp. 132-133.
Scherrer, D., Körner, C., 2011. Topographically controlled thermal-habitat differentiation buffers alpine plant diversity against climate warming. J. Biogeogr. 38, 406–416. https://doi.org/10.1111/j.1365-2699.2010.02407.x.
Schnittler, M., Günther, K.F., 1999. Central European vascular plants requiring priority conservation measures – an analysis from national Red Lists and distribution maps. Biodivers. Conserv. 8, 891–925. https://doi.org/10.1023/a:1008828704456.
Schönswetter, P., Suda, J., Popp, M., Weiss-Schneeweiss, H., Brochmann, C., 2007. Circumpolar phylogeography of *Juncus biglumis* (Juncaceae) inferred from AFLP fingerprints, cpDNA sequences, nuclear DNA content and chromosome numbers. Mol. Phylogenet. Evol. 42, 92–103. https://doi.org/10.1016/j.ympev.2006.06.016.
Schratt-Ehrendorfer L., Niklfeld H., Schröck C., Stöhr O., Hg., 2022: Rote Liste der Farn- und Blütenpflanzen Österreichs. Stapfia 114, Land Oberösterreich, Linz.
Seidl, A., Tremetsberger, K., Pfanzelt, S., Lindhuber, L., Kropf, M., Neuffer, B., Blattner, F. R., Király, G., Smirnov, S.V., Friesen, N., Shmakov, A.I., Plenk, K., Batlai, O., Hurka, H., Bernhardt, K.-G., 2022. Genotyping-by-sequencing reveals range expansion of *Adonis vernalis* (Ranunculaceae) from Southeastern Europe into the zonal Euro-Siberian steppe. Sci. Rep. 12, 19074. https://doi.org/10.1038/s41598-022-23542-w.
Shakun, J.D., Lea, D.W., Lisiecki, L.E., Raymo, M.E., 2015. An 800-kyr record of global surface ocean δ18O and implications for ice volume-temperature coupling. Earth Planet. Sci. Lett. 426, 58–68.
Sheikhakbari-Mehr, R., Maassoumi, A.A., 2017. A note on *Astragalus* L. section *Caprini* DC. Bangladesh Journal of Plant Taxonomy 24, 241. https://doi.org/10.3329/bjpt.v24i2.35122.
Sinaga, P., Klichowska, E., Nowak, A., Nobis, M., 2024. Hybridization and introgression events in cooccurring populations of closely related grasses (Poaceae: *Stipa*) in high mountain steppes of Central Asia. PLoS One 19, e0298760.
Soltis, P.S., Soltis, D.E., 2009. The role of hybridization in plant speciation. Annu. Rev. Plant Biol. 60, 561–588. https://doi.org/10.1146/annurev.arplant.043008.092039.
Sramkó, G., Kosztolányi, A., Laczkó, L., Rácz, R., Szatmári, L., Varga, Z., Barta, Z., 2022. Range-wide phylogeography of the flightless steppe beetle *Lethrus apterus* (Geotrupidae) reveals recent arrival to the Pontic Steppes from the west. Sci. Rep. 12. https://doi.org/10.1038/S41598-022-09007-0.
Stamatakis, A., 2014. RAxML version 8: A tool for phylogenetic analysis and post-analysis of large phylogenies. Bioinformatics 30, 1312–1313. https://doi.org/10.1093/bioinformatics/btu033.
Crvena knjiga flore Srbije 1 – iščezli i krajnje ugroženi taksoni, Ministarstvo za životnu sredinu Republike Srbije, Biološki fakultet Univerziteta u Beogradu, Zavod za zaštitu prirode, 1999. Republike Srbije, Beograd.
Stewart, J.R., Lister, A.M., Barnes, I., Dalén, L., 2010. Refugia revisited: Individualistic responses of species in space and time. Proc. R. Soc. Lond. B: Biol. Sci. 277, 661–671. https://doi.org/10.1098/rspb.2009.1272.
Stojilkovič, V., Záveská, E., Frajman, B., 2022. From western asia to the mediterranean basin: diversification of the widespread *Euphorbia nicaeensis* alliance (Euphorbiaceae). Front. Plant Sci. 13, 815379. https://doi.org/10.3389/fpls.2022.815379.
Strid, A., 2024. Atlas of the Hellenic Flora. Broken Hill Publishers Ltd., Nicosia, pp. 694–700.
Strid, A., Tan, K., 1997. Flora Hellenica. Koeltz Scientific Books, Königstein.
Su, C., Duan, L., Liu, P., Liu, J., Chang, Z., Wen, J., 2021. Chloroplast phylogenomics and character evolution of eastern Asian *Astragalus* (Leguminosae): Tackling the phylogenetic structure of the largest genus of flowering plants in Asia. Mol. Phylogenet. Evol. 156, 107025. https://doi.org/10.1016/J.YMPEV.2020.107025.
Sucháčková Bartoňová, A., Konvička, M., Marešová, J., Kolev, Z., Wahlberg, N., Faltýnek·Fric, Z., 2020. Recently lost connectivity in the Western Palaearctic steppes: the case of a scarce specialist butterfly. Conserv. Genet. 21, 561–575. https://doi.org/10.1007/s10592-020-01271-9.
Suda, J., Trávníček, P., 2006. Estimation of relative nuclear DNA content in dehydrated plant tissues by flow cytometry. In: Robinson, J.P., Darzynkiewicz, Z., Dobrucki, J., Hyun, W., Nolan, J., Orfao, A., Rabinovitch, P. (Eds.), Current Protocols in Cytometry. Wiley, New York. https://doi.org/10.1002/cyto.a.20253, pp. 7.30.1–7.30.14.
Sun, Y., Skinner, D.Z., Liang, G.H., Hulbert, S.H., 1994. Phylogenetic analysis of *Sorghum* and related taxa using internal transcribed spacers of nuclear ribosomal DNA. Theor. Appl. Genet. 89, 26–32. https://doi.org/10.1007/BF00226978.
Surina, B., Schönswetter, P., Schneeweiss, G.M., 2011. Quaternary range dynamics of ecologically divergent species (*Edraianthus serpyllifolius* and *E. tenuifolius*, Campanulaceae) within the Balkan refugium. J. Biogeogr. 38, 1381–1393. https://doi.org/10.1111/j.1365-2699.2011.02493.x.
Sytin, A.K., 2009. Milk-vetches (*Astragalus* L., Fabaceae) of Eastern Europe and the Caucasus: systematics, geography, evolution. D.Sc. Institute of Botany, Russian Academy of Sciences, Saint Petersburg, Russia.
Szabo, K., Pamfil, D., Bădărău, A.S., Hârta, M., 2021. Assessment of genetic diversity and population structure of the endangered *Astragalus exscapus* subsp. *transsilvanicus* through DNA-based molecular markers. Plants 10, 2732.
Talavera, S., Castroviejo, S., 1999. Flora iberica: Plantas vasculares de la Península Ibérica e Islas Baleares: Vol. VII (I) Leguminosae (partim). Editorial CSIC-CSIC Press.
Teso, M.L.R., Parra-Quijano, M., Torres, E., Iriondo, J.M., 2018. Identification and assessment of the crop wild relatives of Spain that require most urgent conservation actions. Mediterr. Bot. 39 (2), 67–75. https://doi.org/10.5209/mbot.60074.
Török, P., Janišová, M., Kuzemko, A., Rūsiņa, S., Stevanović, Z.D., 2018. Grasslands, their threats and management in Eastern Europe. In: Grasslands of the World. CRC Press, pp. 78–102.
Trabelsi, H., Chehma, A., Senoussi, A., Faye, B., Kherraze, M.E., 2023. Camel potentiality in survival and germination of wild pastoral species: The case of Fabaceae in Sahara rangelands of Algeria. J. Arid Environ. 216, 105015.
Tukhbatullin, A., Ermakov, O., Kapustina, S., Starikov, V., Tambovtseva, V., Titov, S., Brandler, O., 2023. Surrounded by kindred: *Spermophilus major* hybridization with other *Spermophilus* species in space and time. Biology 12, 880.
Tutin, T.G., Heywood, V.H., Burges, N.A., Moore, D.M., Valentine, D.H., Walters, S.M., Webb, D.A. (Eds.), 1968. Flora Europaea. Rosaceae to Umbelliferae. Cambridge University Press, Cambridge, p. 469.
Van Der Valk, T., Pečnerová, P., Díez-del-Molino, D., Bergström, A., Oppenheimer, J., Hartmann, S., Xenikoudakis, G., Thomas, J.A., Dehasque, M., Sağlıcan, E., 2021. Million-year-old DNA sheds light on the genomic history of mammoths. Nature 591, 265–269.
Van Geel, B., Aptroot, A., Baittinger, C., Birks, H.H., Bull, I.D., Cross, H.B., Evershed, R. P., Gravendeel, B., Kompanje, E.J.O., Kuperus, P., Mol, D., Nierop, K.G.J., Pals, J.P., Tikhonov, A.N., Van Reenen, G., Van Tienderen, P.H., 2008. The ecological implications of a Yakutian mammoth's last meal. Quat. Res. 69, 361–376. https://doi.org/10.1016/j.yqres.2008.02.004.
Varga, Z., 2010. Extra-mediterranean refugia, post-glacial vegetation history and area dynamics in Eastern Central Europe. In: Relict Species: Phylogeography and Conservation Biology. Springer-Verlag, Berlin Heidelberg, pp. 57–87, 10.1007/978-3-540-92160-8_3.
Wagner, N.D., He, L., Hörandl, E., 2020. Phylogenomic relationships and evolution of polyploid *Salix* species revealed by RAD sequencing data. Front. Plant Sci. 11. https://doi.org/10.3389/fpls.2020.01077.
Wesche, K., Ambarlı, D., Kamp, J., Török, P., Treiber, J., Dengler, J., 2016. The Palaearctic steppe biome: a new synthesis. Biodivers. Conserv. 25, 2197–2231. https://doi.org/10.1007/s10531-016-1214-7.
Wickham, H., Chang, W., Wickham, M.H., 2016. Package 'ggplot2'. Create elegant data visualisations using the grammar of graphics. Version 2 (1), 1–189.
Wilhalm, T., Hilpold, A., 2006. Rote Liste der gefährdeten Gefäßpflanzen Südtirols. Gredleriana 6, 115–198.
Willner, W., Moser, D., Plenk, K., Aćić, S., Demina, O.N., Höhn, M., Kuzemko, A., Roleček, J., Vassilev, K., Vynokurov, D., Kropf, M., 2021. Long-term continuity of steppe grasslands in eastern Central Europe: Evidence from species distribution patterns and chloroplast haplotypes. J. Biogeogr. 48, 3104–3117. https://doi.org/10.1111/jbi.14269.
Wojciechowski, M.F., 2005. *Astragalus* (Fabaceae): A molecular phylogenetic perspective. Brittonia 57, 382–396. https://doi.org/10.1663/0007-196X(2005)057[0382:AFAMPP]2.0.CO;2.
Wojciechowski, M.F., Sanderson, M.J., Hu, J.M., 1999. Evidence on the monophyly of *Astragalus* (Fabaceae) and its major subgroups based on nuclear ribosomal DNA ITS and chloroplast DNA *trnL* intron data. Syst. Bot. 24, 409–437. https://doi.org/10.2307/2419698.
Yuan, J., Sun, G., Xiao, B., Hu, J., Wang, L., Taogetongqimuge, Bao, L., Hou, Y., Song, S., Jiang, S., Wu, Y., Pan, D., Liu, Y., Westbury, M.V., Lai, X., Sheng, G., 2023. Ancient mitogenomes reveal a high maternal genetic diversity of Pleistocene woolly rhinoceros in Northern China. BMC Ecol. Evo. 23, 56. https://doi.org/10.1186/s12862-023-02168-0.
Záveská, E., Maylandt, C., Paun, O., Bertel, C., Frajman, B., The STEPPE Consortium, Schönswetter, P., 2019. Multiple auto- and allopolyploidisations marked the Pleistocene history of the widespread Eurasian steppe plant *Astragalus onobrychis* (Fabaceae). Mol. Phylogenet. Evol. 139. https://doi.org/10.1016/j.ympev.2019.106572.